



DEPARTMENT OF ECONOMICS
AND BUSINESS ECONOMICS
AARHUS UNIVERSITY



Center for Research in Econometric Analysis of Time Series

Explaining Bond Return Predictability in an Estimated New Keynesian Model

Martin Møller Andreasen

CREATES Research Paper 2019-11

Explaining Bond Return Predictability in an Estimated New Keynesian Model*

Martin M. Andreassen[†]

May 22, 2019

Abstract

This paper estimates a New Keynesian model that explains key macro series, the ten-year nominal yield curve, and the ability of the spread between long- and short-term bond yields to predict future excess bond returns. The model also generates an upward sloping nominal and real yield curve, produces a positive inflation risk premium, and recovers the prediction by the expectations hypothesis of no return predictability when historical bond yields are risk-adjusted using term premia from the proposed model. Key to obtaining these results is a new specification of stochastic volatility that allows high current inflation to generate high future uncertainty.

Keywords: Bond return predictability, Term premia, Robust structural estimation, Stochastic volatility.

JEL: E44, G12.

*I thank Kasper Jørgensen, Anders Bredahl Kock, Dennis Kristensen, Giovanni Pellegrino, Morten Ravn, and Daniel Wilhelm for useful comments and discussions. I also appreciate comments from participants at the Cemmap seminar at University College London. I finally acknowledge funding from the Independent Research Fund Denmark, project number 7024-00020B.

[†]Aarhus University, CREATES, and the Danish Finance Institute. Fuglesangs Allé 4, 8210 Aarhus V, Denmark, email: mandreasen@econ.au.dk, telephone +45 87165982.

1 Introduction

One of the most prominent predictors of nominal bond returns is the slope of the yield curve (see Fama and Bliss (1987), Fama and French (1989), Campbell and Shiller (1991), among others). This relationship has been studied extensively in reduced-form dynamic term structure models (DTSMs) using an exogenous pricing kernel with unobserved factors. These models provide a close fit to bond yields but offer little economic intuition. Much effort has therefore been devoted to understanding the economic mechanisms that makes bond returns predictable. For instance, the endowment model of Wachter (2006) emphasizes the importance of time-varying risk aversion from habits, while Bansal and Shaliastovich (2013) stress the importance of fluctuating uncertainty and recursive preferences. However, the insights obtained from these endowment models are restricted by the assumption that both consumption and inflation dynamics are exogenous.

Another strand of the literature relies on dynamic stochastic general equilibrium (DSGE) models with endogenous consumption and inflation dynamics to obtain an even deeper understanding of bond return predictability and term premia in general. For instance, Rudebusch and Swanson (2012) show that recursive preferences and stationary productivity shocks allow the New Keynesian model to match the level and variability of term premia without distorting macro fundamentals. Another important contribution is Kung (2015), who demonstrates that endogenous growth and recursive preferences enable the New Keynesian model to produce term premia dynamics that generate bond return predictability.¹ But so far, DSGE models have not been able to match these unconditional properties of term premia together with the historical evolution in bond yields and key macro variables. Such a requirement to match both unconditional and conditional aspects of the data is satisfied by reduced-form DTSMs and has proven highly valuable, mainly because it gives policy makers and market participants historical estimates of term premia.

Thus, a long-standing ambition in the literature has been to formulate a DSGE model that fits historical bond yields and generates bond return predictability from term premia dynamics that have the same desirable properties as in reduced-form DTSMs. This means that a DSGE model should pass the two requirements in Dai and Singleton (2002) for a

¹Bond return predictability is also studied in the production model of Jermann (2013), which explores the effects of capital investments with multiple sectors in a model with exogenous inflation.

correct specification of term premia. That is, i) reproduce the ability of the spread between long- and short-term bond yields to predict future bond returns as in Campbell and Shiller (1991) and ii) generate no return predictability when historical bond yields are risk-adjusted using term premia from the DSGE model.²

The contribution of the present paper is to address this challenge by proposing a New Keynesian model that i) explains historical bond yields and key macro time series, ii) matches unconditional properties of these variables, and iii) generates term premia dynamics that satisfy the two requirements mentioned above. The key new feature of the proposed model is a modified autoregressive specification of stochastic volatility that allows high current inflation to generate high future uncertainty. We show that this ability of inflation to increase future volatility is present in the reduced-form macro uncertainty measure of Jurado et al. (2015), and that it accounts for the main effects of stochastic volatility in our model. The results show that this link between inflation and uncertainty is essential to generate bond return predictability in the New Keynesian model without distorting macro fundamentals and hence pass the first requirement for a correct specification of term premia. We also demonstrate that this new volatility specification is crucial to meet the second requirement for a correct specification of term premia and ensure no return predictability in historical bond yields when adjusted for term premia. Our analysis reveals that permanent productivity shocks and demand shocks account for most of the variation in nominal term premia and hence explain deviations from the expectations hypothesis in historical bond yields.

To provide additional support for our New Keynesian model, we further show that it matches the level of the upward sloping US yield curve, and that the variability of all bond yields are consistent with the data. The real yield curve is also upward sloping in our model, but by less than for nominal yields, and this generates a positive and upward sloping inflation risk premium. We also find that most of the variation in nominal term premia is due to real term premia, which is consistent with the predictions from the reduced-form DTSMs in Chernov and Mueller (2012) and Abrahams et al. (2016). Taking the analysis beyond bond yields, we finally demonstrate that the proposed New Keynesian model also generates an

²Early contributions that model historical bond yields and macro variables are Graeve et al. (2009) and Bekaert et al. (2010), but they do not allow for time-varying term premia. This feature is incorporated in later models by Binsbergen et al. (2012), Dew-Becker (2014), Amisano and Tristani (2017), Kliem and Meyer-Gohde (2017), and Bianchi et al. (2018), but they do not test the two requirements for a correct specification of term premia.

equity premium of six percent. Here, and throughout we restrict risk aversion to 10 using the formulation of recursive preferences in Andreasen and Jørgensen (forthcoming).

Our analysis is also related to the growing macro literature studying uncertainty shocks in DSGE models (see Justiniano and Primiceri (2008), Fernandez-Villaverde et al. (2011), Fernández-Villaverde et al. (2015), Basu and Bundick (2017), among many others). Here, volatility evolves according to an autoregressive process that is independent of the disturbances to the level of the structural shocks. Given the fairly small effects of uncertainty shocks in most DSGE models, this implies that volatility is only weakly correlated with the business cycle. Our new volatility specification relaxes this assumption and allows for a stronger correlation between uncertainty and the business cycle. Bond market dynamics clearly support this extension of the New Keynesian model, where we find the largest effects of stochastic volatility following ordinary 'level' shocks due to their impact on inflation and subsequently uncertainty. This finding is consistent with the reduced-form evidence in Ludvigson et al. (2019), showing that uncertainty i) reacts endogenously to level shocks and ii) affects the economy by altering the responses of level shocks. Thus, our desire to understand term premia dynamics has revealed a new channel through which inflation and uncertainty affect the economy.

The remainder of this paper is organized as follows. Section 2 presents the classic bond return predictability regression and relates it to DSGE models. Section 3 introduces the New Keynesian model, while our estimation approach is described in Section 4. The main empirical results are provided in Section 5, with robustness checks deferred to Section 6. We finally discuss additional model implications in Section 7 and conclude in Section 8.

2 Bond Return Predictability

A natural starting point for studying bond return predictability is the expectations hypothesis. This hypothesis states that any long-term bond yield is the average of expected future short rates, and that bond returns therefore are unpredictable. Letting $r_t^{(k)}$ denote the k -period bond yield at time t , Campbell and Shiller (1991) suggest to test the expectations hypothesis by regressing the change in the long-term bond yield $r_{t+m}^{(k-m)} - r_t^{(k)}$ on the yield

spread $r_t^{(k)} - r_t^{(m)}$ measuring the slope of the yield curve. That is,

$$r_{t+m}^{(k-m)} - r_t^{(k)} = \alpha_k + \beta_k \frac{m}{k-m} \left(r_t^{(k)} - r_t^{(m)} \right) + u_{t+m,k}, \quad (1)$$

where $u_{t+m,k}$ is an error term. We estimate this regression on US bond yields from 1961 Q2 to 2016 Q2 as provided by Gürkaynak et al. (2007), with $m = 4$ to obtain yearly changes in yields as typically considered (see Cochrane and Piazzesi (2005), Cieslak and Povala (2015), among others). The regressions imply $\beta_8 = -0.74$, $\beta_{20} = -1.55$, and $\beta_{40} = -2.44$ at the two-, five-, and ten-year bond yield, respectively. That is, we obtain the standard finding that β_k is negative and decreasing with maturity, meaning that long-term bond yields tend to fall when the yield spread is high. The expectations hypothesis implies $\beta_k = 1$, which we clearly reject at a 5% significance level (see Figure 2 below). This implies that bond returns are predictable, because (1) is equivalent to running the predictability regression

$$hpr_{t+m}^{(k)} - \frac{m}{4} r_t^{(m)} = \tilde{\alpha}_k + \tilde{\beta}_k \left(r_t^{(k)} - r_t^{(m)} \right) + \varepsilon_{t+m,k},$$

where $hpr_{t+m}^{(k)} \equiv -\frac{k-m}{4} r_{t+m}^{(k-m)} + \frac{k}{4} r_t^{(k)}$ is the holding period return on a k -period bond and $\tilde{\beta}_k \equiv \frac{m}{4} (1 - \beta_k)$.³ Hence, the negative estimates of β_k imply that $\tilde{\beta}_k > 0$, making excess bond returns positively correlated with the yield spread.

The most common explanation for the rejection of the expectations hypothesis is time-varying term premia. A prominent example is Dai and Singleton (2002), which uses the pattern in β_k to select the most appropriate specification of term premia in reduced-form DTSMs. The loadings β_k are unidentified in a first- and second-order perturbation approximation to a DSGE model (where $\beta_k = 1$ by construction), but they become identified when using at least a third-order approximation. Thus, the regression loadings in (1) may also serve as a useful diagnostic tool for DSGE models, because these loadings reveal how the uncertainty corrections in a DSGE model should evolve across the business cycle. The next section exploits this insight to modify a standard macroeconomic model such that its uncertainty corrections and term premia become more flexible as required to match the empirical pattern in β_k .

³The intercept is given by $\tilde{\alpha}_k = -\alpha_k \left(\frac{k}{4} - 1 \right)$.

3 A New Keynesian Model

This section presents a small New Keynesian model for the US economy. The main purpose of this model is to endogenously express consumption and inflation as functions of the structural shocks in the economy, and hence derive a stochastic discount factor from first principles. It is widely acknowledged that the standard version of the New Keynesian model does well in matching aggregate quantities, inflation, and the short rate, but that it struggles to explain asset prices. We therefore augment the New Keynesian model with the flexible formulation of recursive preferences in Andreasen and Jørgensen (forthcoming) and include stochastic volatility. Both extensions have a relatively small effect on aggregate quantities but a sizable effect on inflation and asset prices. We proceed by presenting the decision problem of the households and the firms in Section 3.1 and 3.2, respectively. The behavior of the central bank is outlined in Section 3.3, while our new specification of stochastic volatility is presented in Section 3.4. Section 3.5 computes bond prices and term premia, Section 3.6 presents the model solution, and Section 3.7 discusses properties of term premia at an overall level.

3.1 The Households

We consider an infinitely lived representative household with recursive preferences as in Epstein and Zin (1989) and Weil (1990). Using the formulation in Rudebusch and Swanson (2012), the value function V_t is given by

$$V_t = u_t + \beta \left(\mathbb{E}_t[V_{t+1}^{1-\alpha}] \right)^{1/(1-\alpha)} \quad (2)$$

when the utility function $u_t > 0$ for all t .⁴ Here, $\beta \in (0, 1)$ is the subjective discount factor and $\mathbb{E}_t[\cdot]$ denotes the conditional expectation given information in period t . The main purpose of $\alpha \in \mathbb{R} \setminus \{1\}$ is to endow the household with preferences for when uncertainty is resolved, unless $\alpha = 0$ and (2) reduces to expected utility. Based on Kreps and Porteus (1978), it follows that (2) implies preferences for early (late) resolution of uncertainty if $\alpha > 0$ ($\alpha < 0$) for $u_t > 0$, whereas the opposite sign restrictions apply when $u_t < 0$. Andreasen and

⁴The standard formulation of recursive preferences provided in Epstein and Zin (1989), i.e. $\hat{V}_t = \left[\hat{u}_t^\rho + \beta \left(\mathbb{E}_t[\hat{V}_{t+1}^{\hat{\alpha}}] \right)^{\frac{\rho}{\hat{\alpha}}} \right]^{\frac{1}{\rho}}$, is obtained by letting $V_t = \hat{V}_t^\rho$, $u_t = \hat{u}_t^\rho$, and $\hat{\alpha} = \rho(1 - \alpha)$. For $u_t < 0$, we define $V_t = u_t - \beta \mathbb{E}_t[(-V_{t+1})^{1-\alpha}]^{\frac{1}{1-\alpha}}$ as in Rudebusch and Swanson (2012).

Jørgensen (forthcoming) further argue that the size of this timing attitude is proportional to α , meaning that numerically larger values of α generate stronger preferences for early (late) resolution of uncertainty.

The utility function $u_t \equiv u(c_t, l_t)$ is assumed to depend on the number of consumption units c_t bought in the goods market and the provided labor supply l_t to firms. Following Andreasen and Jørgensen (forthcoming), we also include a constant u_0 in the utility function to account for utility from goods and services that are not acquired in the goods market. This could be utility from government spending or utility from goods produced and consumed within the household. As shown in Andreasen and Jørgensen (forthcoming), the main reason for introducing u_0 is to separately control the level of the utility function and hence disentangle the timing attitude from relative risk aversion (RRA), which otherwise are tightly linked in the standard formulation of recursive preferences. Using a power specification to quantify the utility from market consumption c_t and similarly for leisure $1 - l_t$, we let

$$u(c_t, l_t) = d_t \left[\frac{1}{1-\chi} c_t^{1-\chi} + z_t^{1-\chi} n_t \varphi_0 \frac{(1-l_t)^{1-\frac{1}{\varphi}}}{1-\frac{1}{\varphi}} + u_0 z_t^{1-\chi} \right]. \quad (3)$$

Here, d_t is a preference shock, which temporally increases or decreases the utility from a given level of c_t and l_t , implying that d_t operates as a demand shock. The variable n_t is also exogenous and temporally shifts the household's incentive between c_t and l_t , meaning that n_t may be interpreted as a labor supply shock. Market consumption grows with the rate of the productivity level z_t , and it is therefore necessary to scale the utility from leisure and nonmarket consumption by $z_t^{1-\chi}$ to ensure that these terms do not diminish relative to $\frac{1}{1-\chi} c_t^{1-\chi}$ along the balanced growth path. This scaling is discussed and motivated further in Rudebusch and Swanson (2012) and Andreasen and Jørgensen (forthcoming).⁵

The parameter $\chi > 0$ determines the intertemporal elasticity of substitution (IES) as $1/\chi$, which measures the percentage change in market consumption growth for a one percent change in the real interest rate when ignoring uncertainty. The Frisch labor supply elasticity with respect to the real wage is $\varphi \left(\frac{1}{l_t} - 1 \right)$ and therefore mainly determined by $\varphi > 0$. The endogenous labor supply gives the household an additional margin to absorb shocks and this modifies existing expressions for RRA. Using the results in Swanson (2018), it follows that

⁵Our results are robust to restricting $u_0 = 0$ as in the standard implementation of recursive preferences, provided one allows for high RRA (see Section 6.3).

RRA in the steady state (ss) is given by

$$\text{RRA} = \frac{\chi}{1 + \chi \varphi \frac{\tilde{w}_{ss}(1-l_{ss})}{\tilde{c}_{ss}}} + \frac{\alpha(1-\chi)}{(1-\chi) u_0 \tilde{c}_{ss}^{\chi-1} + 1 + \frac{1-\chi}{1-\frac{1}{\varphi}} \frac{\tilde{w}_{ss}(1-l_{ss})}{\tilde{c}_{ss}}},$$

where $\tilde{c}_{ss} = c_t/z_t|_{ss}$ and $\tilde{w}_{ss} = w_t/z_t|_{ss}$ refer to the steady state of market consumption and the real wage relative to the productivity level. Given that the IES is determined by χ and that α controls the strength of the timing attitude, the level of the utility function u_0 is the key parameter for determining RRA, as shown in Andreasen and Jørgensen (forthcoming).

The real budget constraint for the household is $c_t + \mathbb{E}_t [M_{t,t+1} X_{t+1}] = \frac{X_t}{\pi_t} + w_t l_t + D_t$. That is, resources are spent on market consumption goods c_t and nominal state-contingent claims X_{t+1} , which are priced using the nominal stochastic discount factor $M_{t,t+1}$. The household's income is given by the real value of state-contingent claims bought in the previous period X_t/π_t , the real wage income $w_t l_t$, and real dividend payments from firms D_t . Here, π_t denotes the gross inflation rate.

The first-order conditions for the utility maximizing household are

$$\mathbb{E}_t [M_{t,t+1} e^{r_t}] = 1 \quad (4)$$

$$z_t^{1-\chi} n_t \varphi_0 (1-l_t)^{-\frac{1}{\varphi}} = c_t^{-\chi} w_t, \quad (5)$$

where r_t is the net one-period nominal risk-free interest rate. Equation (4) is the well-known consumption-Euler equation, while (5) is the optimality condition for the labor supply.

3.2 The Firms

Output y_t is produced by a perfectly competitive representative firm, which combines differentiated intermediate goods $y_t(i)$ using $y_t = \left(\int_0^1 y_t(i)^{\frac{\eta-1}{\eta}} di \right)^{\frac{\eta}{\eta-1}}$ with $\eta > 1$. The demand for the i th good is given by $y_t(i) = \left(\frac{P_t(i)}{P_t} \right)^{-\eta} y_t$, where $P_t \equiv \left(\int_0^1 P_t(i)^{1-\eta} di \right)^{\frac{1}{1-\eta}}$ denotes the aggregate price level and $P_t(i)$ is the price of the i th good.

Intermediate firms produce slightly differentiated goods using $y_t(i) = z_t a_t k_{ss}^\theta l_t(i)^{1-\theta}$, where k_{ss} and $l_t(i)$ denote capital and labor services at the i th firm, respectively. The variable a_t captures transitory productivity shocks, while z_t specifies the long-term growth

path for the productivity level. Both a_t and z_t are taken to be exogenous and specified below in Section 3.4. Each intermediate firm can freely adjust its labor demand at the given market wage w_t . Price stickiness is introduced as in Rotemberg (1982), where $\xi \geq 0$ controls the size of firms' real cost $\frac{\xi}{2} (P_t(i) / (P_{t-1}(i) \pi_{ss}) - 1)^2 y_t$ when changing the optimal nominal price $P_t(i)$ of the good they produce. As in Rudebusch and Swanson (2012), each firm uses $\delta k_{ss} z_t$ units of output for investment to maintain a constant capital stock along the balanced growth path of the economy. The first-order conditions for profit maximization are

$$w_t = mc_t (1 - \theta) z_t a_t k_{ss}^\theta l_t^{-\theta} \quad (6)$$

$$y_t (1 - \eta) + \mathbb{E}_t \left[\xi M_{t,t+1} \pi_{t+1} \left(\frac{\pi_{t+1}}{\pi_{ss}} - 1 \right) \frac{\pi_{t+1}}{\pi_{ss}} y_{t+1} \right] + mc_t y_t \eta = \xi \left(\frac{\pi_t}{\pi_{ss}} - 1 \right) y_t \frac{\pi_t}{\pi_{ss}}, \quad (7)$$

where mc_t denotes marginal costs. Equation (6) determines labor demand, and (7) implies an aggregate supply relation between output and inflation.

The resource constraint reads $c_t + z_t \delta k_{ss} = \left(1 - \frac{\xi}{2} \left(\frac{\pi_t}{\pi_{ss}} - 1 \right)^2 \right) y_t$, where $\frac{\xi}{2} \left(\frac{\pi_t}{\pi_{ss}} - 1 \right)^2 y_t$ is the output loss from price stickiness.

3.3 The Central Bank

The central bank sets the one-period nominal interest rate r_t as

$$r_t = r_{ss} + \phi_{\pi,t} \log \left(\frac{\pi_t}{\pi_{ss}} \right) + \phi_y \log \left(\frac{y_t}{z_t \tilde{y}_{ss}} \right), \quad (8)$$

based on a desire to close the inflation and the output gap. Note that the inflation gap is defined relative to steady state inflation π_{ss} , and that the output gap is expressed as y_t in deviation from its level along the balanced growth path $z_t \tilde{y}_{ss}$, where $\tilde{y}_{ss} = y_t / z_t|_{ss}$. To accommodate deviations in monetary policy from a simple Taylor-rule, we follow Fernández-Villaverde and Rubio-Ramirez (2008), Ang et al. (2011), among others and allow for a time-varying coefficient $\phi_{\pi,t}$ in the Federal Reserve's response to the inflation gap. A relatively high value of $\phi_{\pi,t}$ captures episodes where the Federal Reserve is mostly focused on stabilizing the inflation gap, whereas a relatively low value of $\phi_{\pi,t}$ represents episodes with more focus on the output gap. Variation in $\phi_{\pi,t}$ is taken to be exogenous and specified below.

3.4 The Structural Shocks

We index the five structural shocks in the model by x_t , i.e. $x_t \in \{\mu_{z,t}, n_t, d_t, \phi_{\pi,t}, a_t\}$ where $\mu_{z,t} \equiv z_t/z_{t-1}$ is the gross growth rate in the productivity level. The adopted specification of a shock with stochastic volatility σ_t is given by

$$\log x_t = v_{x,t}\sigma_t, \quad (9)$$

where $v_{x,t+1}$ evolves as

$$v_{x,t+1} = \rho_x v_{x,t} + \sigma_x \varepsilon_{x,t+1}, \quad (10)$$

with $|\rho_x| < 1$ and $\sigma_x \geq 0$. The innovation $\varepsilon_{x,t}$ is assumed to be normal and independently distributed across time, i.e. $\varepsilon_{x,t} \sim \mathcal{NID}(0, 1)$. Leading (9) by one period and inserting (10), it follows that

$$\log x_{t+1} = \rho_x \frac{\sigma_{t+1}}{\sigma_t} \log x_t + \sigma_{t+1} \sigma_x \varepsilon_{x,t+1}. \quad (11)$$

Thus, (11) is nearly identical to the standard volatility specification in the literature, except for the persistence coefficient $\rho_x \sigma_{t+1}/\sigma_t$ that replaces ρ_x (see Fernández-Villaverde and Rubio-Ramírez (2007), Justiniano and Primiceri (2008), among others). This difference is not essential for our application, where σ_{t+1}/σ_t remains close to one for all periods.⁶ The main advantage of the volatility specification in (9) and (10) is that it only requires one extra state ($v_{x,t}$) per shock in the model, whereas the traditional specification of stochastic volatility induces two additional states ($\log x_{t-1}$ and $\varepsilon_{x,t}$). This state reduction greatly helps to keep the proposed model simple and suitable for estimation.

The considered process for σ_t is given by

$$\sigma_{t+1} = \sigma_{ss} (1 - \rho_\sigma) + \rho_\sigma \sigma_t + \gamma_\pi \left(\log \left(\frac{\pi_t}{\pi_{ss}} \right) - \mathbb{E} \left[\log \left(\frac{\pi_t}{\pi_{ss}} \right) \right] \right) + \sigma_\sigma \varepsilon_{\sigma,t+1}, \quad (12)$$

where $|\rho_\sigma| < 1$, $\gamma_\pi \in \mathbb{R}$, $\sigma_\sigma \geq 0$, and $\varepsilon_{\sigma,t+1} \sim \mathcal{NID}(0, 1)$. The first two terms are standard, whereas the third term represents our key extension. As in the traditional specification of σ_t , the innovation $\varepsilon_{\sigma,t}$ is independent of $\{\varepsilon_{\mu_z,t}, \varepsilon_{n,t}, \varepsilon_{d,t}, \varepsilon_{\phi_\pi,t}, \varepsilon_{a,t}\}$, which also display mutually independence. Thus, volatility is centered around $\sigma_{ss} > 0$ and has an autoregressive

⁶For instance, our preferred specification in Section 5 implies that σ_{t+1}/σ_t rarely goes outside the interval $[0.96, 1.04]$.

component $\rho_\sigma \sigma_t$ to capture the persistent nature of uncertainty. The traditional specification of stochastic volatility simply adds $\sigma_\sigma \varepsilon_{\sigma,t+1}$ to these two terms, making σ_t independent of the structural shocks hitting the economy. Given the fairly small effects of uncertainty shocks in most New Keynesian models, this makes σ_t weakly correlated with the business cycle. The purpose of the new term $\gamma_\pi \left(\log \left(\frac{\pi_t}{\pi_{ss}} \right) - \mathbb{E} \left[\log \left(\frac{\pi_t}{\pi_{ss}} \right) \right] \right)$ in (12) is to relax this assumption and accommodate the possibility that uncertainty is more closely related to the business cycle. The use of inflation to capture the link between uncertainty and the business cycle is mainly motivated by the work of Coibion and Gorodnichenko (2011). They show that higher steady state inflation in the New Keynesian model makes indeterminacy and hence erratic variation in macro variables more likely. Thus, Coibion and Gorodnichenko (2011) establish a positive relation between the long-term inflation rate and macroeconomic uncertainty, which we extend to more short-term business cycle dynamics when $\gamma_\pi > 0$.

The unconditional mean $\mathbb{E}[\log(\pi_t/\pi_{ss})]$ is approximated by the auxiliary variable aux_t , which captures the mean of $\log(\pi_t/\pi_{ss})$ that is different from zero in a nonlinear approximation. Following Andreasen et al. (2018), we let $aux_t = (1 - \gamma) \mathbb{E}_t \left[\sum_{k=0}^{\infty} \gamma^k \log \left(\frac{\pi_{t+k}}{\pi_{ss}} \right) \right]$ with $\gamma = 0.99995$, which ensures that aux_t is basically constant at the mean of $\log(\pi_t/\pi_{ss})$.

3.5 Bond Pricing

The presence of state contingent claims imply that all financial assets in the economy can be priced using standard no-arbitrage arguments. Thus, the price in period t of a default-free zero-coupon bond $B_t^{(k)}$ maturing in k periods with a face value of one dollar is $B_t^{(k)} = \mathbb{E}_t \left[M_{t,t+1} B_{t+1}^{(k-1)} \right]$ for $k = 1, \dots, N$ with $B_t^{(0)} = 1$. With continuous compounding, the corresponding yield to maturity is $r_t^{(k)} = -\frac{1}{k} \log B_t^{(k)}$, where $r_t^{(1)} \equiv r_t$. Bond prices are therefore entirely determined by the nominal stochastic discount factor as given by

$$M_{t,t+1} = \beta \frac{d_{t+1}}{d_t} \left(\frac{c_{t+1}}{c_t} \right)^{-\chi} \left(\frac{(\mathbb{E}_t [V_{t+1}^{1-\alpha}])^{\frac{1}{1-\alpha}}}{V_{t+1}} \right)^\alpha \frac{1}{\pi_{t+1}} \quad (13)$$

when $u_t > 0$ for all t .⁷ The first term $\beta d_{t+1}/d_t$ is the subjective discount factor adjusted for demand shocks. The second term is the well-known ratio of future to current marginal

⁷When $u_t < 0$ for all t , V_{t+1} is replaced by $-V_{t+1}$ in (13).

utility of market consumption $(c_{t+1}/c_t)^{-\alpha}$. The third term is due to recursive preferences and amplifies the effect of unexpected changes in household utility as measured by the value function. This function summarizes current and future utility, implying that the expected future level of market consumption, leisure, and non-market consumption affect bond prices when $\alpha \neq 0$.

To study the implied bond risk premia, we follow Rudebusch and Swanson (2012), Adrian et al. (2013), among others and define term premium $TP_t^{(k)}$ as the difference between $r_t^{(k)}$ and the corresponding yield under risk-neutral pricing $\tilde{r}_t^{(k)}$. That is, $TP_t^{(k)} = r_t^{(k)} - \tilde{r}_t^{(k)}$ where $\tilde{r}_t^{(k)} = -\frac{1}{k} \log \tilde{B}_t^{(k)}$ and $\tilde{B}_t^{(k)} = e^{-r_t} \mathbb{E}_t [\tilde{B}_{t+1}^{(k-1)}]$ with $\tilde{B}_t^{(0)} = 1$.

3.6 Model Solution

The state vector for this model is given by $\mathbf{x}_t = [\sigma_t \ v_{\mu_z,t} \ v_{n,t} \ v_{d,t} \ v_{\phi_\pi,t} \ v_{a,t}]'$, where only σ_t is endogenous. All the remaining variables appear in \mathbf{y}_t , including the labor supply, consumption, inflation, and all bond prices. The exact solution to the model is

$$\begin{aligned} \mathbf{y}_t &= \mathbf{g}(\mathbf{x}_t, \sigma; \boldsymbol{\theta}) \\ \mathbf{x}_{t+1} &= \mathbf{h}(\mathbf{x}_t, \sigma; \boldsymbol{\theta}) + \sigma \boldsymbol{\eta} \boldsymbol{\varepsilon}_{t+1}, \end{aligned} \tag{14}$$

where $\boldsymbol{\varepsilon}_t = [\varepsilon_{\sigma,t} \ \varepsilon_{\mu_z,t} \ \varepsilon_{n,t} \ \varepsilon_{d,t} \ \varepsilon_{\phi_\pi,t} \ \varepsilon_{a,t}]'$ and $\boldsymbol{\theta}$ denotes the structural parameters. The auxiliary parameter $\sigma \geq 0$ scales $\boldsymbol{\eta}$, which contains the standard deviations to $\boldsymbol{\varepsilon}_t$. The functions $\mathbf{g}(\cdot)$ and $\mathbf{h}(\cdot)$ are not available in closed form and approximated by a third-order perturbation solution to accommodate time-varying term premia. This is done by first using invariant transformations to obtain an equivalent representation of the model without the trending variables V_t , c_t , w_t , y_t , and z_t . For instance, (2) and (13) are expressed in terms of the scaled value function $\tilde{V}_t \equiv V_t/z_t^{1-\alpha}$ and scaled consumption $\tilde{c}_t \equiv c_t/z_t$. The third-order approximation is then computed for this transformed version of the model at the steady state, i.e. at $\mathbf{x}_t = \mathbf{x}_{t+1} = \mathbf{x}_{ss}$ and $\sigma = 0$.⁸

⁸For an efficient implementation, we use the codes of Binning (2013) to compute the third-order approximation to a special version of the model without bond prices exceeding one period. All remaining bond prices and bond risk premia are computed afterwards using the method of Andreasen and Zabczyk (2015).

3.7 Properties of Term Premia

Although the perturbation method does not analytically show how θ affects derivatives of $\mathbf{g}(\cdot)$ and $\mathbf{h}(\cdot)$, it is still informative to analyze the approximation of term premia at an overall level. To do so, recall that the third-order perturbation approximation to $\mathbf{g}(\cdot)$ is

$$\mathbf{y}_t = \mathbf{y}_{ss} + \mathbf{g}_x \hat{\mathbf{x}}_t + \frac{1}{2} \mathbf{g}_{xx} (\hat{\mathbf{x}}_t \otimes \hat{\mathbf{x}}_t) + \frac{1}{6} \mathbf{g}_{xxx} (\hat{\mathbf{x}}_t \otimes \hat{\mathbf{x}}_t \otimes \hat{\mathbf{x}}_t) + \frac{1}{2} \mathbf{g}_{\sigma\sigma} + \frac{1}{2} \mathbf{g}_{\sigma\sigma x} \hat{\mathbf{x}}_t, \quad (15)$$

where $\hat{\mathbf{x}}_t \equiv \hat{\mathbf{x}}_t - \mathbf{x}_{ss}$ and subscripts on $\mathbf{g}(\cdot)$ denote derivatives evaluated at the steady state for a given value of θ . The derivatives \mathbf{g}_x , \mathbf{g}_{xx} , and \mathbf{g}_{xxx} represent a third-order approximation to the deterministic version of the model. Given that term premia are zero in the absence of uncertainty, it follows that rows in \mathbf{y}_t which represent term premia have zero loadings in \mathbf{g}_x , \mathbf{g}_{xx} , and \mathbf{g}_{xxx} as noted in Andreasen (2012). Hence, a third-order perturbation approximation to term premia in our model is simply

$$TP_t = \frac{1}{2} \mathbf{g}_{\sigma\sigma}^{TP} + \frac{1}{2} \mathbf{g}_{\sigma\sigma x}^{TP} \hat{\mathbf{x}}_t \quad (16)$$

where $\mathbf{g}_{\sigma\sigma}^{TP}$ and $\mathbf{g}_{\sigma\sigma x}^{TP}$ represent the entries in $\mathbf{g}(\cdot)$ for term premia. This shows that term premia are linear (i.e. affine) in the states as typically assumed in reduced-form DTSMs following Duffee (2002). However, the parametric restrictions on term premia in these reduced-form models are clearly less restrictive than in our New Keynesian model with a stochastic discount factor derived from first principles.

Our second observation is that $\mathbf{g}_{\sigma\sigma}$ and $\mathbf{g}_{\sigma\sigma x}$ correct for variance risk, and that the conditional variance of the state innovations $\boldsymbol{\eta}\boldsymbol{\eta}'$ enter linearly in the equations determining $\mathbf{g}_{\sigma\sigma}$ and $\mathbf{g}_{\sigma\sigma x}$ (see Schmitt-Grohé and Uribe (2004) and Andreasen (2012), respectively). Thus, one way for the New Keynesian model to avoid the well-known problem of too low and stable term premia is to increase the conditional variance $\boldsymbol{\eta}\boldsymbol{\eta}'$ because it amplifies $\mathbf{g}_{\sigma\sigma}$ and $\mathbf{g}_{\sigma\sigma x}$. But an excessive level of $\boldsymbol{\eta}\boldsymbol{\eta}'$ has the drawback of generating too much volatility in bond yields and aggregate quantities, as emphasized in Rudebusch and Swanson (2008).

A popular way to avoid this variance trade-off in the New Keynesian model is to introduce recursive preferences. These preferences enter through a Jensen's inequality effect on the value function, meaning that they only affect $\mathbf{g}_{\sigma\sigma}$ and $\mathbf{g}_{\sigma\sigma x}$ in (15). This property of recursive preferences greatly helps to increase the flexibility of term premia, and allows the New

Keynesian model to match the level and variability of term premia without distorting macro fundamentals, as shown in Rudebusch and Swanson (2012).

Extending the New Keynesian model with stochastic volatility adds further flexibility to term premia, because it mainly affects the approximation solution through $\mathbf{g}_{\sigma\sigma}$ and $\mathbf{g}_{\sigma\sigma\mathbf{x}}$. For the traditional specification of stochastic volatility, this additional flexibility is primarily obtained by making σ_t an extra state variable in the expression for term premia. As shown in Andreasen (2012), this may greatly increase the variability of term premia without distorting macro fundamentals. But the weak correlation between σ_t and the business cycle does not help to control the comovement of term premia with macro fundamentals and the yield spread, as summarized by the predictability result in Section 2. The extension of stochastic volatility that we propose in (12) through γ_π alleviates this constraint by making σ_t comove with macro fundamentals. As we will show below, this comovement of σ_t adds valuable flexibility to term premia and enables the New Keynesian model to satisfy the two requirements for a correct specification of term premia.

4 Estimation Methodology

This section describes how we estimate the New Keynesian model. We proceed by presenting our data in Section 4.1, outline the adopted estimation routine in Section 4.2, and discuss the calibrated values for the parameters that are not estimated in Section 4.3.

4.1 Data

We estimate the model using quarterly US data from 1961 Q2 to 2016 Q2. The dynamics of the macro economy is represented by i) labor supply $\log l_t$, ii) consumption growth Δc_t , and iii) inflation.⁹ The ten-year nominal yield curve is represented by the three-month, one-year, three-year, five-year, seven-year, and ten-year bond yield. These yields are taken from Gürkaynak et al. (2007), except at the three-month maturity where we use the implied rate

⁹The labor supply is measured by the average weekly hours of production and nonsupervisory employees in the manufacturing sector, normalized by 5×24 to match the definition of labor in our model. The consumption growth rate is calculated from real per capita nondurables and service expenditures. Inflation is measured by the year-on-year growth rate in the consumer price index (CPI) for all urban consumers. All three data series are downloaded from the Federal Reserve Bank of St. Louis.

on a three-month Treasury Bill. These nine time series are placed in the vector \mathbf{y}_t^{obs} and expressed in annualized terms except for $\log l_t$.

4.2 Robustified Inference with Nonlinear Filtering

The model solution in Section 3.6 includes nonlinear terms with the unobserved state vector \mathbf{x}_t , implying that the Kalman filter cannot be used to estimate the model. Instead, we rely on the central difference Kalman filter (CDKF) developed by Norgaard et al. (2000), which is a nonlinear extension of the Kalman filter. The CDKF accommodates measurement errors in \mathbf{y}_t^{obs} , and these errors \mathbf{v}_t are specified to be uncorrelated Gaussian white noise, as typically assumed when estimating DSGE models and reduced-form DTSMs (see, for instance, Fernández-Villaverde and Rubio-Ramírez (2007) and Joslin et al. (2011), respectively). That is, $\mathbf{v}_t \sim \mathcal{NID}(\mathbf{0}, \mathbf{R}_v)$ where \mathbf{R}_v is a diagonal matrix. Unlike particle filters, the updating rule for the states in the CDKF is restricted to have a linear functional form, implying that the recursive filtering equations only depend on first and second moments. The CDKF approximates these moments by a deterministic sampling procedure, and this makes the CDKF computationally much faster than any particle filter and generally also more accurate than the well-known extended Kalman filter.

A likelihood function can be derived from the CDKF under the assumption that the prediction errors for \mathbf{y}_t^{obs} are Gaussian. However, this distributional specification does not hold exactly due to the nonlinear terms in the model solution. The CDKF therefore only provides a quasi log-likelihood function $\frac{1}{T} \sum_{t=1}^T \mathcal{L}_t(\boldsymbol{\theta})$, which can be used for a quasi maximum likelihood (QML) estimation, as suggested in Andreasen (2013).

A possible limitation of any QML approach (as with standard maximum likelihood) is its lack of robustness to model misspecifications other than the distributional assumption of the prediction errors for \mathbf{y}_t^{obs} , in particular without priors to regularize the likelihood function as shown in Ruge-Murcia (2007). An obvious possible source of misspecification in our case is that \mathbf{v}_t may not be uncorrelated Gaussian white noise, but may contain cross-correlation, auto-correlation, and outliers. One way to account for cross- and auto-correlation in \mathbf{v}_t is to follow Ireland (2004) and use a vector autoregressive model for \mathbf{v}_t inside the CDKF. Unfortunately, this procedure introduces a lot of extra unknown parameters in our case with nine observables. We want to avoid such an extension of the parameter space, and

we therefore suggest a computationally less demanding alternative. The simple idea behind our procedure is to consider a set of unconditional moments that are unaffected by the aforementioned misspecifications in \mathbf{v}_t and then shrink the QML estimates towards these more robust moments. The main benefit of this procedure to robustify a likelihood-based estimator is that no additional parameters are introduced, and that unconditional moments are easy to compute for DSGE models. We denote these shrinkage moments by $\frac{1}{T} \sum_{t=1}^T \mathbf{m}_t$ in the sample and by $\mathbb{E}[\mathbf{m}(\boldsymbol{\theta})]$ in the model. Hence, the considered estimator is given by

$$\hat{\boldsymbol{\theta}} = \arg \max_{\boldsymbol{\theta} \in \Theta} \frac{1}{T} \sum_{t=1}^T \mathcal{L}_t(\boldsymbol{\theta}) - \lambda \mathbf{g}_{1:T}(\boldsymbol{\theta})' \mathbf{W} \mathbf{g}_{1:T}(\boldsymbol{\theta}) \quad (17)$$

where Θ is the feasible domain of $\boldsymbol{\theta}$, $\mathbf{g}_{1:T}(\boldsymbol{\theta}) \equiv \frac{1}{T} \sum_{t=1}^T \mathbf{g}_t(\boldsymbol{\theta})$ with $\mathbf{g}_t(\boldsymbol{\theta}) \equiv \mathbf{m}_t - \mathbb{E}[\mathbf{m}(\boldsymbol{\theta})]$, and \mathbf{W} is a diagonal weighting matrix containing the inverse of the standard errors for the shrinkage moments.¹⁰

The nature of the estimator in (17) is determined by $\lambda \geq 0$, which controls the weight assigned to the shrinkage moments relative to the sample average of $\mathcal{L}_t(\boldsymbol{\theta})$. We obviously recover the standard QML estimator when $\lambda = 0$, while $\hat{\boldsymbol{\theta}}$ converges to the generalized methods of moments (GMM) estimator in Hansen (1982) when λ becomes sufficiently large. We will generally consider a small amount of shrinkage by letting $\lambda = T$, which in our setting implies that shrinkage constitutes a fairly small part of the objective function, typically about 5% to 10%. Our results are not particularly sensitive to increasing the degree of shrinkage further, although we do find notable effects of shrinkage when compared to the standard QML estimator with $\lambda = 0$.¹¹

To ensure closed-form expressions for the model-implied shrinkage moments, we apply the pruning scheme of Andreasen et al. (2018) when setting up the state space system for the approximated version of the New Keynesian model.¹² This implies that our new

¹⁰Another possibility is to use the optimal weighing matrix, but this version of (17) is not considered to avoid well-known small-sample distortions from estimating large co-variance matrices in moment-based estimators (see, for instance, Smith (1993)).

¹¹It may also be informative to note that (17) belongs to the class of Laplace type or quasi-Bayesian estimators of Chernozhukov and Hong (2003), where a potentially misspecified log-likelihood function (as considered in our case) may be used within a Bayesian setting. When this estimator is combined with the endogenous prior specification in Christiano et al. (2011) using a pre-sample of length T^* , we obtain the objective function in (17) with $\lambda = T^*/2$.

¹²The pruning scheme is not essential in our case, because the considered model has only one endogenous state (σ_t), and partly for this reason appears to be stable when simulated without the pruning scheme.

estimator can be implemented without resorting to simulation and belongs to the general class of extremum estimators, as summarized in Hayashi (2000). Its asymptotic properties are therefore easily derived in Appendix A.1. Hence, for a sufficiently large sample T , one may expect $\hat{\boldsymbol{\theta}}$ to be normally distributed around its true value and with the covariance matrix

$$Var(\hat{\boldsymbol{\theta}}) = \frac{1}{T} \mathbf{A}^{-1} Var(\mathbf{q}_t) \mathbf{A}^{-1}.$$

Here, $\mathbf{q}_t \equiv -\mathbf{s}_t(\boldsymbol{\theta}) + 2\lambda \mathbf{G}(\boldsymbol{\theta})' \mathbf{W} \mathbf{g}_t(\boldsymbol{\theta})$ is the score function for observation t when accounting for shrinkage, where $\mathbf{s}_t(\boldsymbol{\theta}) \equiv \partial \mathcal{L}_t(\boldsymbol{\theta}) / \partial \boldsymbol{\theta}$ denotes the score of the quasi log-likelihood function in period t and $\mathbf{G}(\boldsymbol{\theta}) \equiv \partial \mathbf{g}_{1:T}(\boldsymbol{\theta}) / \partial \boldsymbol{\theta}'$ is the Jacobian for the shrinkage moments. The matrix \mathbf{A} denotes the Hessian of $\hat{\boldsymbol{\theta}}$ and is estimated by

$$\hat{\mathbf{A}} = 2\lambda \mathbf{G}(\hat{\boldsymbol{\theta}})' \mathbf{W} \mathbf{G}(\hat{\boldsymbol{\theta}}) - \frac{1}{T} \sum_{t=1}^T \mathbf{H}_t(\hat{\boldsymbol{\theta}}).$$

Here, $\mathbf{H}_t(\boldsymbol{\theta}) \equiv \partial \mathbf{s}_t(\boldsymbol{\theta}) / \partial \boldsymbol{\theta}'$ refers to the Hessian of \mathcal{L}_t , which we compute using first-order numerical derivatives of \mathcal{L}_t as in Harvey (1989). The score function \mathbf{q}_t will generally display autocorrelation and heteroskedasticity, and its variance $Var(\mathbf{q}_t)$ is therefore obtained using the estimator in Newey and West (1987) with a bandwidth of 10 lags.

We use two classes of shrinkage moments. The first class contains first and second unconditional moments of \mathbf{y}_t^{obs} . These moments are unaffected by the aforementioned misspecifications in \mathbf{v}_t and helps to robustify the QML estimates. This is illustrated in a Monte Carlo study in Appendix A.2, where shrinkage towards these moments generally give smaller parameter biases and more reliable inference than standard QML when \mathbf{v}_t contains cross-correlation, auto-correlation, and outliers but the quasi log-likelihood function is computed with $\mathbf{v}_t \sim \mathcal{NID}(\mathbf{0}, \mathbf{R}_v)$. When \mathbf{v}_t is uncorrelated Gaussian white noise as assumed in the CDKF, we unexpectedly find no benefit of shrinkage. Here, shrinkage mainly reduces the efficiency of the standard QML estimator, which nearly is unbiased and provide reliable inference in this case.

The second class of moments we consider capture the information in the Campbell-Shiller regression loadings at the three-, five-, and ten-year maturity, and hence assigns more weight to the evidence against the expectations hypothesis than implied by the considered panel of bond yields used to compute the quasi log-likelihood function. For these loadings, we include

both the covariance $Cov(r_{t+m}^{(k-m)} - r_t^{(k)}, r_t^{(k)} - r_t^{(m)})$ and the variance $Var(r_t^{(k)} - r_t^{(m)})$ related to β_k in (1) at the three considered maturities.

4.3 Calibrated Parameters

Not all parameters in the New Keynesian model are well-identified from \mathbf{y}_t^{obs} , and they are therefore determined by standard calibration arguments as commonly done in the literature (see Christiano et al. (2005), Justiniano and Primiceri (2008), among others). Hence, we let $\delta = 0.025$ and $\theta = 0.4$ as typically assumed for the US economy. We also consider an average price markup of 20% with $\eta = 6$, and we set the ratio of capital to output in the steady state to 2.5 as in Rudebusch and Swanson (2012). The value of $\mu_{z,ss}$ is set to match the mean of consumption growth, implying that $\mu_{z,ss} = 1.0049$. For the volatility process, we normalize the mean of σ_t to one by letting $\sigma_{ss} = 1$, which generally also ensures that σ_t stays positive when simulating the estimated versions of the New Keynesian model reported below. The sticky price parameter ξ is badly identified, and we therefore use a linear version of our model to set ξ to match a Calvo parameter of $\alpha_p = 0.75$, giving an average duration for prices of four quarters.¹³ Most micro estimates of the Frisch labor supply elasticity for males are in the range from 0.10 to 0.40 according to Keane (2011). To help the New Keynesian model generate low variability in the labor supply, we consider a Frisch elasticity in the lower part of this interval by letting $\varphi = 0.075$, which implies a Frisch elasticity of about 0.15 in the steady state.

Given this calibration of φ and our finding below that χ is larger than one, the utility function in (3) is negative. Hence, the parameter α characterizing the recursive preferences in (2) must be negative to generate preferences for early resolution of uncertainty. The model's goodness of fit generally improves the more negative α gets, but the performance gain trails off when α gets below -60 in our case.¹⁴ We therefore simply let $\alpha = -60$, which imply that a third-order perturbation solution delivers a reasonable accurate approximation as shown in Appendix B. This value of α also ensures a low and plausible level of the timing premium as introduced in Epstein et al. (2014). We finally set the constant u_0 to get a steady state RRA of 10 as in Bansal and Yaron (2004).

¹³The mapping is $\xi = ((1 - \theta + \eta\theta)(\eta - 1)\alpha_p) / \left((1 - \alpha_p)(1 - \theta) \left(1 - \alpha_p\beta\mu_{z,ss}^{1-\frac{1}{\psi}} \right) \right)$.

¹⁴Rudebusch and Swanson (2012) report a similar property of recursive preferences in their model.

The size of the measurement errors in \mathbf{y}_t^{obs} have a relatively small effect on the estimates, and we therefore simply assume that 10% of the variation in the three macro variables is due to measurement errors.¹⁵ This implies measurement errors with standard deviations of i) 17 basis points for $\log l_t$, ii) 18 basis points for consumption growth, and iii) 29 basis points for inflation. The standard deviation for the measurement errors in all bond yields is set to 15 basis points, which corresponds to 5% of the average standard deviations in the six considered bond yields.

5 Estimation Results

This section presents the main results for our preferred specification of the New Keynesian model. We proceed by discussing the estimated parameters and the model fit in Section 5.1, while stylized unconditional moments are reported in Section 5.2. The model-implied Campbell-Shiller regression loadings are examined in Section 5.3, and the model's ability to explain deviations from the expectations hypothesis in these regressions is studied in Section 5.4. The estimated term premium is provided in Section 5.5. We finally explain the key mechanisms of the model in Section 5.6, and study the model's implications for conditional heteroskedasticity in Section 5.7.

5.1 Estimated Parameters and Model Fit

The first column in Table 1 reports the estimated model parameters in our preferred version of the New Keynesian model. This model is denoted $\mathcal{M}^{M,CS}$, where the superscripts indicate that shrinkage is applied based on the first and second unconditional moments of \mathbf{y}_t^{obs} (by "M") and the selected Campbell-Shiller moments (by "CS"). For the utility of consumption, we find $\hat{\chi} = 6.67$, which implies an IES of 0.15. This relatively low IES is consistent with Hall (1988), Barsky et al. (1997), and Yogo (2004), which estimate the IES to be between zero and 0.2. We also find a realistic timing premium of 9%, meaning that the household is willing to give up 9% of total lifetime consumption to have all uncertainty resolved in the following period. The timing premium is here computed as in Andreasen and Jørgensen (forthcoming).

¹⁵A similar assumption is used in An and Schorfheide (2007), which assume that 20% of the variation in the data can be assigned to measurement errors.

Permanent productivity shocks are found to be highly persistent ($\hat{\rho}_{\mu_z} = 0.973$) and with small innovations ($\hat{\sigma}_{\mu_z} = 3.4 \times 10^{-4}$), meaning that $\mu_{z,t}$ captures long-run risk as in Bansal and Yaron (2004). We also find that $\hat{\gamma}_\pi = 4.46$ with a tight standard error of 0.475, meaning that γ_π is different from zero at all conventional significance levels. Thus, the proposed extension of the volatility specification in (12) is strongly supported by the data, showing that high inflation generates high future uncertainty. The central bank is found to assign more weight to stabilizing inflation than economic activity with $\hat{\phi}_\pi = 6.93$ and $\hat{\phi}_y = 0.03$. Although this is a common finding, the value of ϕ_π is somewhat higher than typically reported in the literature. However, re-estimating the model with $\gamma_\pi = 0$ reduces $\hat{\phi}_\pi$ to 3.86 according to Table 1. This shows that the positive link between inflation and uncertainty, which we propose in this paper, gives the central bank a stronger incentive to stabilize inflation and hence uncertainty.¹⁶

Figure 1 plots the data and the model-implied time series by black and red lines, respectively. We generally find a very close fit to the three macro variables and the six bond yields. This is also evident from Table 2, showing that the standard deviations for the measurement errors in bond yields are between 8 and 24 basis points, and hence comparable to standard three-factor reduced-form DTSMs. For instance, Cheridito et al. (2007) report model errors with standard deviations between 10 and 27 basis points. The bottom part of Table 2 further shows that the applied shrinkage in $\mathcal{M}^{M,CS}$ has a small effect on the optimal value of the objective function, where the GMM moment conditions only account for about 6% (i.e. 1.9/33.4) of its value.

5.2 Unconditional Stylized Moments

Table 3 explores the ability of $\mathcal{M}^{M,CS}$ to match several stylized unconditional moments for the US economy. The first column in Table 3 shows US sample moments (and their bootstrapped 95% confidence bands), while the second column shows the corresponding population moments in $\mathcal{M}^{M,CS}$. We first note that $\mathcal{M}^{M,CS}$ reproduces the mean level of the three macro variables and all bond yields. For instance, the level of the three-month yield is 4.89% vs. 4.76% in the data, and the level of the ten-year bond yield is 6.25% vs. 6.35% in

¹⁶Without stochastic volatility, unreported results show that the weight assigned to the inflation gap falls further to 3.52, which is close to the estimate of 3.14 reported in Andreasen et al. (2018) for a New Keynesian model with homoskedastic shocks approximated to third order.

the data. This implies that the average yield spread is 136 basis points in $\mathcal{M}^{M,CS}$ compared to 159 basis points in the sample.

Our New Keynesian model is also successful in matching the standard deviation of inflation (1.93% vs. 1.79% in the data) and consumption growth (2.87% vs. 2.91% in the data). For all bond yields, $\mathcal{M}^{M,CS}$ generates slightly more volatility than seen in the data, but the model-implied standard deviations are all within the 95% confidence bands for the sample moments. For the labor supply, the standard deviation is 2.53%, which is slightly larger than the empirical standard deviation of 1.72% and its upper 95% confidence bound of 2.02%. Subject to this minor qualification, $\mathcal{M}^{M,CS}$ is also able to explain the unconditional variability in the data.

5.3 Bond Return Predictability

We next explore if $\mathcal{M}^{M,CS}$ can reproduce the observed degree of return predictability in US bond yields by matching the empirical pattern of the Campbell-Shiller loadings. Figure 2 plots these loadings in the sample along with their bootstrapped 95% confidence bands. The corresponding model-implied loadings are computed in closed form using the population moments of $\mathcal{M}^{M,CS}$. The very encouraging finding is that $\mathcal{M}^{M,CS}$ generates Campbell-Shiller loadings that are *negative* and *decreasing* with maturity, and hence tract the empirical loadings remarkably well inside their 95% confidence bands. This shows that our New Keynesian model satisfies the first requirement for a correct specification of term premia.

Figure 2 also reveals that removing the impact of inflation on volatility by imposing $\gamma_\pi = 0$ has a dramatic effect in the model. For this restricted version of $\mathcal{M}^{M,CS}$, the Campbell-Shiller loadings are *positive* and *increase* with maturity. That is, the complete opposite pattern compared to the full model and the data. This shows that our extension with inflation affecting volatility through γ_π is essential for $\mathcal{M}^{M,CS}$ to reproduce the desired degree of return predictability in US bond yields.

5.4 Risk-Adjusted Campbell-Shiller Regressions

The second requirement for a correct specification of term premia is that risk-adjusted historical bond yields satisfy the expectations hypothesis. Dai and Singleton (2002) show that this corresponds to testing whether the slope coefficient β_k^{Adj} is equal to one in a version of

the Campbell-Shiller regression, where term premia are subtracted from long-term yields as follows

$$\begin{aligned} & r_{t+m}^{(k-m)} - r_t^{(k)} - \left(\widetilde{TP}_{t+m}^{(k-m)} - \widetilde{TP}_t^{(k-m)} \right) + \frac{m}{k-m} TP_t^{fwd, (k-m)} \\ &= \alpha_k^{Adj} + \beta_k^{Adj} \frac{m}{k-m} \left(r_t^{(k)} - r_t^{(m)} \right) + u_{t+m, k}^{Adj}. \end{aligned} \quad (18)$$

Here, $\widetilde{TP}_t^{(k)} = r_t^{(k)} - \frac{1}{k} \sum_{i=0}^{k-1} \mathbb{E}_t [r_{t+i}]$ is another commonly used definition of term premium, that only differs from $TP_t^{(k)}$ by including a small convexity term. The variable $TP_t^{fwd, (k)} = f_{t, k} - \mathbb{E}_t [r_{t+k}]$ is the term premium in the forward rate $f_{t, k} \equiv -\log (B_{t, k+1}/B_{t, k})$ and $u_{t+m, k}^{Adj}$ is an error term.

Figure 3 uses term premia from $\mathcal{M}^{M, CS}$ to compute the risk-adjusted Campbell-Shiller loadings β_k^{Adj} and their 95% confidence bands on the historical sample of bond yields from 1961 Q2 to 2016 Q2. Very encouragingly, we find that all these loadings are close to one, and that the 95% confidence bands for these estimates always contain the desired value of one. Thus, we are no longer able to reject the expectations hypothesis for historical bond yields once they are risk-adjusted. This shows that term premia from our New Keynesian model are not rejected by data, and hence also passes the second requirement for a correct specification of term premia.

Figure 3 also shows that omitting the effect of inflation on volatility by letting $\gamma_\pi = 0$ has a strong effect on β_k^{Adj} . For this restricted version of $\mathcal{M}^{M, CS}$, the risk-adjusted Campbell-Shiller loadings are negative beyond the two year maturity and strongly decreasing with maturity. Thus, we clearly violate the expectations hypothesis for risk-adjusted long-term bond yields when $\gamma_\pi = 0$.¹⁷ This shows that the proposed extension of σ_t in (12), where volatility depends on inflation, is essential for the New Keynesian model to generate plausible term premia dynamics and explain the observed deviations from the expectations hypothesis.

5.5 Nominal Term Premia

The ten-year term premium implied by $\mathcal{M}^{M, CS}$ is shown in Figure 4, where the shaded bars denote NBER recessions. The figure reveals that our New Keynesian model generates the

¹⁷Unreported results show that β_k^{Adj} is significantly different from one at the 5% level for maturities exceeding four years.

same overall pattern for nominal term premia as observed in the flexible five-factor model of Adrian et al. (2013), which is a standard reduced-form DTSM without any economic structure imposed on the stochastic discount factor. The correlation between the two measures of term premia is 77%, with the similarities being particularly strong after the mid 1980s. Most of the observed differences between the two models appear around NBER recessions, where the New Keynesian model tends to generate more counter-cyclical variation in term premia than seen in the reduced-form model of Adrian et al. (2013). This difference is also evident from simple summary statistics, as $\mathcal{M}^{M,CS}$ implies a ten-year nominal term premium with a mean of 184 basis points and a standard deviation of 179 basis points, while the corresponding figures are 168 and 123 basis points, respectively, for the reduced-form model of Adrian et al. (2013).

5.6 Understanding the Key Mechanisms in the Model

At this point, we have shown that the proposed model i) explains historical bond yields, ii) matches unconditional properties of yields, and iii) passes the two requirements for a correct specification of term premia. These aspects of the data are also matched by reduced-form DTSMs, but this class of models offers little insights into the economic mechanisms that determine bond yields and especially term premia dynamics. The New Keynesian we propose in this paper provides such a structural explanation, and this section analyzes some of the key mechanisms in $\mathcal{M}^{M,CS}$ that drive term premia. Our discussion is structured around Table 4, which shows how unconditional moments and Campbell-Shiller loadings (both ordinary and risk-adjusted) are affected when omitting one of the six shocks in the model.

First, permanent productivity shocks have a large effect in the model. This is seen clearly from the unconditional means in Table 4, where omitting variation in $\mu_{z,t}$ (i.e. $\sigma_{\mu_z} = 0$) generates a strong steepening of the yield curve. For instance, the three-month bond yield falls from 4.89% to -0.27% and the ten-year bond yield increases from 6.25% to 20.90%. That is, a permanent productivity shock generates a negative term premium. To understand why, observe from Figure 5 that a positive shock to $\mu_{z,t}$ increases consumption, reduces labor, and raises inflation. We therefore see a fall in the stochastic discount factor $M_{t,t+1}$ that coincides with a fall in the long-term nominal bond price $B_t^{(40)}$. As shown in Rudebusch and

Swanson (2012), such a positive comovement between $M_{t,t+1}$ and $B_t^{(40)}$ generates a negative term premium, and this explains why permanent productivity shocks help to flatten the yield curve. Table 4 also shows that permanent productivity shocks account for much of the variation in medium- and long-term bond yields. For instance, the standard deviation in $r_t^{(40)}$ falls from 3.61% to 1.86% when letting $\sigma_{\mu_z} = 0$. We also find that ordinary Campbell-Shiller loadings increase without permanent technology shocks, for instance from -1.3 to -0.7 for $r_t^{(40)}$. This shows that permanent technology shocks also play an important role in generating bond return predictability in $\mathcal{M}^{M,CS}$. The risk-adjusted Campbell-Shiller loadings are also strongly affected when $\sigma_{\mu_z} = 0$, as all estimates of β_k^{Adj} are negative, although not significantly different from one due to the wide confidence bands.

Second, the fifth column in Table 4 shows that we get a strongly inverted yield curve without demand shocks (i.e. $\sigma_d = 0$), meaning that these shocks help to generate an *upward* sloping yield curve in $\mathcal{M}^{M,CS}$. In contrast, demand shocks typically generate a downward sloping yield curve in the New Keynesian model (see, for instance, Nakata and Tanaka (2016)). To understand this implication of $\mathcal{M}^{M,CS}$, observe that a positive demand shock increases consumption, reduces labor, and raises inflation in Figure 6. Despite these responses, we see a temporary *increase* in the stochastic discount factor, because d_t also scales the constant u_0 in the utility function. This generates a large increase in the value function V_{t+1} , which translates into a positive spike in the stochastic discount factor through the term $(\mathbb{E}_t [V_{t+1}^{1-\alpha}])^{\frac{\alpha}{1-\alpha}} / V_{t+1}^\alpha$ in (13). Thus, we have a negative comovement between $M_{t,t+1}$ and the bond price $B_t^{(40)}$, implying that demand shocks carry a positive term premium in $\mathcal{M}^{M,CS}$.

Third, the fifth column in Table 4 also shows a large positive increase in ordinary Campbell-Shiller loadings when imposing $\sigma_d = 0$. For instance, β_{40} increases from -1.3 to 0.2 when omitting demand shocks. We do not observe a similar positive increase in the ordinary Campbell-Shiller loadings when abstracting from any of the other shocks, implying that demand shocks are the main driver behind bond return predictability in $\mathcal{M}^{M,CS}$. To further clarify which feature in $\mathcal{M}^{M,CS}$ that helps to generate bond return predictability, consider once again the impulse response functions following a positive demand shock in Figure 6. Here, we find a fall in the expected long-term bond yield, i.e. $\mathbb{E}_t [r_{t+4}^{(36)}] - r_t^{(40)}$, and a steeping of the yield spread $r_t^{(40)} - r_t^{(4)}$, as required to get a negative Campbell-Shiller loading. Figure 6 also shows that this steeping of the yield spread is absent if we momentarily impose $\gamma_\pi = 0$ to get the standard volatility specification. That is, we only experience the

required increase in long-term bond yields because higher inflation generates higher volatility in $\mathcal{M}^{M,CS}$. Note also that the same volatility response from inflation generates the negative comovement between $\mathbb{E}_t \left[r_{t+4}^{(36)} \right] - r_t^{(40)}$ and $r_t^{(40)} - r_t^{(4)}$ in Figure 5 following a permanent productivity shock. Taken together, this shows that the proposed extension in (12), where σ_t depends on inflation through γ_π , constitutes a new important channel for generating bond return predictability in the New Keynesian model.

Finally, the second column in Table 4 reveals that the effects of not including exogenous shocks to volatility (i.e. $\sigma_\sigma = 0$) are fairly small, as all the unconditional moments are nearly identical to those reported for the full model. Hence, the main effects of stochastic volatility in $\mathcal{M}^{M,CS}$ come from the response of σ_t following a productivity shock, a demand shock, or other 'level' shocks as captured by γ_π . This property of our New Keynesian model is thus consistent with the reduced-form evidence in Ludvigson et al. (2019), showing that uncertainty reacts endogenously to level shocks and affects the economy by altering the responses of level shocks.

5.7 Decomposing Conditional Heteroskedasticity

It is well-known that the nonlinear structure of the New Keynesian model generates time-variation in the conditional second moments even with homoskedastic shocks (see, for instance, Rudebusch and Swanson (2012)). In $\mathcal{M}^{M,CS}$, this endogenous source of conditional heteroskedasticity is captured by the nonlinearities in the \mathbf{g} -function in (14). But we also allow for stochastic volatility in the states through σ_t , and this generates an additional source of conditional heteroskedasticity. Given the importance of time-varying volatility for generating bond return predictability and plausible term premia dynamics in general, it is informative to examine how much of the conditional heteroskedasticity in $\mathcal{M}^{M,CS}$ is endogenously generated and how much can be assigned to the process for σ_t .

To address this question, let $\sigma_{\mathbf{y}^{obs},t}$ denote the conditional standard deviation of \mathbf{y}_{t+1}^{obs} given \mathbf{x}_t . Based on the pruned third-order perturbation approximation, we then use the results in Andreasen et al. (2018) to compute $\sigma_{\mathbf{y}^{obs},t}$ in closed form at a given state. The first column in Table 5 reports the standard deviation of $\sigma_{\mathbf{y}^{obs},t}$ in a simulated sample. Imposing $\gamma_\pi = 0$ in $\mathcal{M}^{M,CS}$ reduces the variability in the conditional standard deviations by 40% to 50% for Δc_t and all bond yields, while we see smaller changes for the labor supply and

inflation. The effects of also imposing $\sigma_\sigma = 0$ (such that $\sigma_t = \sigma_{ss}$) are much smaller, with the largest change appearing for the three-month yield that decreases from -49% to -60% compared to $\mathcal{M}^{M,CS}$ with only $\gamma_\pi = 0$.

We draw two conclusions from these simulations. First, the new mechanism we propose by introducing γ_π in (12) accounts for 40% to 50% of the conditional heteroskedasticity in Δc_t and bond yields. In contrast, the effects of the traditional exogenous volatility shocks via $\sigma_\sigma \varepsilon_{\sigma,t+1}$ are much smaller in $\mathcal{M}^{M,CS}$. Second, between 40% to 60% of the conditional heteroskedasticity in Δc_t and bond yields remain endogenously generated in the New Keynesian model even when introducing stochastic volatility.

6 Robustness Analysis

This section examines the robustness of our main results in Section 5. We first consider the effects of shrinkage in Section 6.1, while the New Keynesian model is re-estimated with $\gamma_\pi = 0$ in Section 6.2 and $u_0 = 0$ in Section 6.3. Section 6.4 finally presents reduced-form evidence that supports a volatility response from inflation as captured by $\gamma_\pi > 0$.¹⁸

6.1 The Effects of Shrinkage

To assess the impact of shrinkage, we first re-estimate the New Keynesian model when only shrinking the QML estimates to the first and second unconditional moments of \mathbf{y}_t^{obs} and not to the Campbell-Shiller loadings. This version of the New Keynesian model is denoted \mathcal{M}^M . We find that this modification has a small effect on the estimated structural parameters in Table 1, the model fit in Table 2, and the unconditional means in Table 3. For the unconditional standard deviations, \mathcal{M}^M provides a slightly closer fit to the data with less variability in labor and most bond yields when compared to $\mathcal{M}^{M,CS}$. Table 6 shows that \mathcal{M}^M also generates bond return predictability with Campbell-Shiller loadings close to -0.7 , although these loadings are somewhat lower (in absolute terms) than in $\mathcal{M}^{M,CS}$ and the data. On the other hand, \mathcal{M}^M implies risk-adjusted Campbell-Shiller loadings that are even closer to the desired value of one than in $\mathcal{M}^{M,CS}$. Thus, our New Keynesian model remains able to

¹⁸In the online appendix, we further show that our results in Section 5 are robust to i) ending the estimation in 2007 Q4, ii) doubling the standard deviations for the measurement errors, iii) decreasing α to -80 , and iiiii) increasing the degree of shrinkage by letting $\lambda = T \times 10$ in (17).

generate bond return predictability and explain deviations from the expectations hypothesis, even when omitting ordinary Campbell-Shiller loadings from the shrinkage moments.

Another possibility is to abstract from any shrinkage and simply use QML for the estimation. We refer to this version of the New Keynesian model as \mathcal{M} . Table 1 shows that this modification results in somewhat larger changes in the estimated structural parameters. As expected, we also find that these estimates give a closer in-sample fit, with \mathcal{M} having smaller measurement errors for nearly all series when compared to $\mathcal{M}^{M,CS}$ and \mathcal{M}^M (see Table 2). However, an important limitation of not applying shrinkage is shown in Table 3, as \mathcal{M} generates too high bond yields. Their unconditional mean exceeds 8%, which is well outside the wide 95% confidence bands for the empirical level of the US yield curve. Another shortcoming of \mathcal{M} is the elevated level of the standard deviations in labor and most bond yields, which typically also exceed their upper 95% confidence bounds. Thus, the improved in-sample fit of the New Keynesian model when estimated without shrinkage comes at the cost of distorting the fit to several unconditional properties of the model, and this seems highly undesirable.

6.2 The Volatility Specification

The novel feature of our New Keynesian model is the response in volatility to changes in inflation. This link is captured by γ_π , which generates bond return predictability and explains deviations from the expectations hypothesis, as shown above. We next re-estimate the New Keynesian model with $\gamma_\pi = 0$ to explore whether the model is able to generate bond predictability and plausible term premia dynamics without this novel link between volatility and inflation. This restricted version of the New Keynesian model is denoted $\mathcal{M}_{\gamma_\pi=0}^{M,CS}$ when estimated with the full degree of shrinkage.

Table 1 shows that imposing $\gamma_\pi = 0$ has notable effects on the estimated structural parameters, with β increasing from 0.967 to 0.985, ϕ_π falling from 6.93 to 3.86, and higher persistence in several shocks ($\mu_{z,t}$, n_t , and a_t) than seen in $\mathcal{M}^{M,CS}$. The in-sample fit worsens in general when imposing $\gamma_\pi = 0$, as we find larger measurement errors for labor, consumption growth, and all bond yields according to Table 2. The unconditional means and the ordinary Campbell-Shiller loadings in Table 6 remain well matched with $\gamma_\pi = 0$, but Table 3 also shows that the variability in labor and long-term bond yields are now too high. For

instance, the standard deviation in labor is 5.05% vs. 1.72% in the data, and the standard deviation in the ten-year bond yield is 4.08%, which exceeds the corresponding sample moment of 2.70% and its 95% upper confidence bound of 3.76%. Table 6 also shows that all risk-adjusted Campbell-Shiller loadings for $\mathcal{M}_{\gamma_\pi=0}^{M,CS}$ are negative and statistically different from one at the 5% level. Thus, the restricted model $\mathcal{M}_{\gamma_\pi=0}^{M,CS}$ cannot explain the observed deviations from the expectations hypothesis and is therefore unable to satisfy the second requirement for a correct specification of term premia.

It is also informative to estimate this restricted version of the New Keynesian model without shrinking towards the ordinary Campbell-Shiller loadings. This version of the New Keynesian model $\mathcal{M}_{\gamma_\pi=0}^M$ gives clearly a better in-sample fit than $\mathcal{M}_{\gamma_\pi=0}^{M,CS}$, and it matches both the level and variability of bond yields, although the standard deviation in labor remains too high. Importantly, $\mathcal{M}_{\gamma_\pi=0}^M$ does not match the ordinary Campbell-Shiller loadings, which are positive and increasing with maturity, as shown in Table 6. At the ten-year maturity, we even have that $\mathcal{M}_{\gamma_\pi=0}^M$ reproduces the expectations hypothesis ($\beta_{40} \approx 1.0$) and hence does not generate any bond return predictability. Another sign of misspecification is seen in the risk-adjusted Campbell-Shiller loadings for $\mathcal{M}_{\gamma_\pi=0}^M$, which are negative and statistically different from one at the 5% level.

Thus, when $\gamma_\pi = 0$, the New Keynesian model struggles to match various unconditional properties of the data and is unable to explain the historical deviations from the expectations hypothesis, i.e. pass the second requirement for a correct specification of term premia.

6.3 The Standard Formulation of Recursive Preferences

We have so far used the flexible formulation of recursive preferences in Andreasen and Jørgensen (forthcoming) by including the constant u_0 in the utility function to disentangle the timing attitude from RRA. We next impose $u_0 = 0$ to consider the standard formulation of recursive preference with a tight link between the timing attitude and RRA. This restricted version of the New Keynesian model is denoted $\mathcal{M}_{u_0=0}^{M,CS}$ when estimated with the full degree of shrinkage.

Unreported results show that the fit of this restricted model improves for lower values of α , and we therefore let $\alpha = -60$ for comparability with the unrestricted model $\mathcal{M}^{M,CS}$. Table 1 shows that imposing $u_0 = 0$ has a very small effect on the estimated structural

parameters, although we find lower persistence in the labor supply shocks n_t and smaller demand shocks d_t when compared to $\mathcal{M}^{M,CS}$. However, risk aversion is substantially higher when $u_0 = 0$ with $RRA = 217$, whereas it is only 10 in all the other versions of the model. Table 2 shows that the in-sample fit as measured by log-likelihood function is unaffected by imposing $u_0 = 0$, whereas the model’s ability to match the shrinkage moments improves slightly from -1.9 in $\mathcal{M}^{M,CS}$ to -1.8 in $\mathcal{M}_{u_0=0}^{M,CS}$. This improvement is mainly due to a lower standard deviation for the labor supply of 1.72%, which now perfectly matches the corresponding sample moment (see Table 3). We further observe from Table 6 that $\mathcal{M}_{u_0=0}^{M,CS}$ generates similar ordinary Campbell-Shiller loadings as in $\mathcal{M}^{M,CS}$ and explains historical deviations from the expectations hypothesis with β_k^{Adj} close to one.

We draw two conclusions from these results. First, restricting RRA to 10 is accompanied by a small reduction in model’s ability to match the data when using the recursive preferences of Andreasen and Jørgensen (forthcoming). Second, the New Keynesian model is also able to match the data with the standard formulation of recursive preferences, provided one is willing to accept a high RRA – perhaps to proxy for model uncertainty or omitted household heterogeneity as mentioned in Rudebusch and Swanson (2012).

6.4 Reduced-Form Evidence of Inflation Induced Volatility

All the structural estimates of γ_π in Table 1 are highly significant, showing that a positive relationship between volatility and inflation helps the New Keynesian model match postwar US data. To provide some external validation for this relationship, we next use the monthly macro uncertainty index of Jurado et al. (2015) ending in April 2015 to directly estimate (12) by ordinary least squares (OLS).

The left part of Table 7 follows the specification in (12) closely and regresses σ_{t+1} on a constant, σ_t , and CPI inflation. The residuals display evidence of auto-correlation, and the standard errors are therefore computed as in Newey and West (1987) using a bandwidth of six lags. For the full sample, we find that $\hat{\gamma}_\pi$ is positive and significant at the 5% level. Restricting the sample to start in 1990 does not alter this finding, as $\hat{\gamma}_\pi$ remains positive and has a p -value of 5.11% for the null hypothesis of $\gamma_\pi = 0$.¹⁹ Thus, the positive relationship

¹⁹The volatility measure in Jurado et al. (2015) has a different scale compared to σ_t in the New Keynesian model, implying that the magnitude of the reduced-form estimates of γ_π in Table 7 is not directly comparable to the structural estimates in Table 1.

between volatility and inflation holds even when ignoring the 1970s and 1980s. The right part of Table 7 introduces an additional lag of volatility compared to the previous regression model to eliminate any auto-correlation in the residuals. For the full sample and the reduced sample starting in 1990 we once again find that $\hat{\gamma}_\pi$ is positive and significant at the 5% level.

Thus, the clear message from these simple reduced-form regressions is that high current inflation coincides with high future volatility, as also implied by our structural estimates in Table 1.

7 Additional Model Implications

This section studies additional asset pricing implications of $\mathcal{M}^{M,CS}$ and relates our findings to the existing literature. We first show in Section 7.1 which structural shocks control the level, slope, and curvature of the yield curve to offer an economic explanation behind variation in the factors applied in many reduced-form DTSMs. A structural decomposition of nominal term premia is carried out in Section 7.2 to examine the economic forces that determine risk premia in the bond market. To provide further support for our New Keynesian model, we then show that it also matches the level of real bond yields and the inflation risk premium in Section 7.3, and that it explains the high equity premium in Section 7.4.

7.1 Level, Slope, and Curvature

It well-known that nearly all cross-sectional variation in bond yields can be captured by three factors representing level, slope, and curvature of the yield curve. Reduced-form DTSMs in the tradition of Joslin et al. (2011) use these factors to elegantly explain the evolution in the yield curve, but this modeling approach has the disadvantage of being silent about the economic forces driving bond yields. In contrast, our New Keynesian model uses structural shocks to explain bond yields, and we are therefore able to study the economic forces determining the level, slope, and curvature of the yield curve.

To address this question, Figure 7 shows the impulse response functions for the three yield-factors to each of the structural shocks in $\mathcal{M}^{M,CS}$. The three yield-factors are here defined as in Diebold et al. (2006), i.e. $\mathcal{L}_t^r \equiv (r_t^{(40)} + r_t^{(8)} + r_t)/3$ for level, $\mathcal{S}_t^r \equiv r_t^{(40)} - r_t$ for slope, and $\mathcal{C}_t^r \equiv 2r_t^{(8)} - r_t - r_t^{(40)}$ for curvature. The top row of Figure 7 shows that permanent

productivity shocks $v_{\mu_z,t}$ and shocks to the Taylor rule $v_{\phi_\pi,t}$ have the largest impact on the level factor, but that demand shocks $v_{d,t}$ also play an important role. When regressing \mathcal{L}_t^r on a constant, $v_{\mu_z,t}$, and $\phi_{\pi,t}$ in a simulated sample of 100,000 observations, the explained variation is $R^2 = 82\%$. If we also add demand shocks to this regression, then R^2 increases to 93%. Adding the three remaining shocks to the regression takes R^2 to 97%, implying that only 3% of the variation in \mathcal{L}_t^r is due to nonlinearities in the \mathbf{g} -function in (15).

The middle row in Figure 7 shows that demand shocks $v_{d,t}$ are the key driver of the slope factor, and that this effect only arises from the positive link between inflation and volatility as captured by γ_π . Thus, regressing \mathcal{S}_t^r on a constant and $v_{d,t}$ in a simulated sample of 100,000 observations gives an R^2 of 67%. We also note that shocks to volatility σ_t have a large impact on \mathcal{S}_t^r , and adding σ_t to the regression takes R^2 to 76%, whereas $R^2 = 80\%$ when including all six shocks. This implies that 20% of the variation in \mathcal{S}_t^y is due to the nonlinear terms $\mathbf{x}_t \otimes \mathbf{x}_t$ and $\mathbf{x}_t \otimes \mathbf{x}_t \otimes \mathbf{x}_t$ in (15), meaning that the slope factor displays stronger nonlinearities in comparison with the level factor.

For the curvature factor in the bottom row of Figure 7, we find that permanent productivity shocks $v_{\mu_z,t}$, demand shocks $v_{d,t}$, and shocks to the Taylor rule $v_{\phi_\pi,t}$ are the most important disturbances. Regressing \mathcal{C}_t^r on a constant, $v_{\mu_z,t}$, $v_{d,t}$, and $v_{\phi_\pi,t}$ in a simulated sample of 100,000 observations gives an R^2 of 45%, which only increases to 54% when including all six shocks. Thus, nonlinearities constitute a very large proportion of the variation in the curvature factor (46%), and this may explain why it is hard to find good observable proxies for \mathcal{C}_t^r (see, for instance, Diebold et al. (2006))

A principal component analysis for the six bond yields in \mathbf{y}_t^{obs} on US data shows that \mathcal{L}_t^r explains 97.31% of the variation in bond yields, while it is 2.42% for \mathcal{S}_t^r and 0.22% for \mathcal{C}_t^r . These ratios are closely matched by $\mathcal{M}^{M,CS}$ in a simulated sample of 100,000 observations, as the corresponding figures are 97.36%, 2.42%, and 0.12% for \mathcal{L}_t^r , \mathcal{S}_t^r , and \mathcal{C}_t^r , respectively. Thus, our structural model provides the same cross-sectional split of the variation in bond yields as observed in the data, although each of the reduced-form factors is explained by *several* structural shocks in the New Keynesian model.

7.2 Decomposing Nominal Term Premium

One of the main advantages of a structural model is the economic interpretation attached to each shock, meaning that the model offers a deeper understanding of the mechanisms driving term premia than available in more reduced-form models. Such an analysis is provided in Figure 8, which uses (16) to perform a shock decomposition of nominal term premium. This figure shows that the ten-year nominal term premium is mainly driven by permanent productivity shocks $v_{\mu_z,t}$ and demand shocks $v_{d,t}$, which account for 41% and 49% of the total variation in term premium, respectively. A careful inspection of Figure 8 reveals that $v_{\mu_z,t}$ tends to be high and $v_{d,t}$ low just before the start of a recession. During recessions, we generally see a fall in productivity $v_{\mu_z,t}$ but also a sequence of positive demand shocks that increase the level of $v_{d,t}$. This fall in $v_{\mu_z,t}$ has a negative effect on term premium, whereas the higher value of $v_{d,t}$ increases term premium. Figure 8 shows that the latter effect generally dominates, and this explains why term premium peaks at the end or immediately after recessions in the US. The only exceptions are the two recessions in the early 1980s, where we generally see the opposite pattern in $v_{\mu_z,t}$ and $v_{d,t}$.

7.3 The Real Yield Curve and the Inflation Risk Premium

We next explore whether our New Keynesian model can match the level of real bond yields. For the three-month real interest rate r_t^{real} , we find that $\mathbb{E}[r_t^{real}] = 0.89\%$ in $\mathcal{M}^{M,CS}$, which is in line with the estimates typically reported in the literature. For instance, the mean of the real interest rate is 0.86% in Bansal and Yaron (2004) and 0.94% in Campbell and Cochrane (1999). We also find that the level of real bond yields increases with maturity in $\mathcal{M}^{M,CS}$, with the ten-year real bond yield $r_t^{real,(40)}$ having an unconditional mean of 2.14%. This level is consistent with the results of Chernov and Mueller (2012), where $\mathbb{E}[r_t^{real,(40)}]$ is between 1.93% and 2.75%, depending on whether yields on Treasury inflation protected securities are included in the estimation of their reduced-form DTSM. Unreported results show that this upward sloping real yield curve in $\mathcal{M}^{M,CS}$ is generated by demand shocks, and the mechanism is identical to the one described above for the nominal yield curve. The only difference compared to nominal yields is that real bond prices are not affected by inflation and therefore display a weaker response to demand shocks than seen for nominal bond prices. The negative covariance between the stochastic discount factor and any real bond price is

therefore lower (in absolute terms) when compared with the corresponding nominal bond price, and this explains why the real yield curve has a lower unconditional slope (125 basis points) than the nominal yield curve (136 basis points) in $\mathcal{M}^{M,CS}$. These results ensure that the real term premium $TP_t^{real,(k)}$ in $\mathcal{M}^{M,CS}$ is also increasing with maturity. At the ten-year maturity, its unconditional mean is 159 basis points, while its standard deviation is 154 basis points.

It is also informative to explore the model's implication for the inflation risk premium, which is given by the difference between the nominal and real term premium, i.e. $TP_t^{(k)} - TP_t^{real,(k)}$. For $\mathcal{M}^{M,CS}$ we find that the inflation risk premium is increasing with maturity, having a mean of 25 basis points and a standard deviation of 25 basis points at the ten-year maturity. Thus, most of the level and variation in the nominal term premium in our New Keynesian model are due to real term premia, which is consistent with the predictions from the reduced-form DTSMs in Chernov and Mueller (2012) and Abrahams et al. (2016).

7.4 The Equity Premium

Another way to assess the performance of the proposed model is to explore its ability to explain the high equity premium in the US. We define equity as a claim on D_t^ω , where D_t is firm dividends and ω accounts for leverage. This implies that the real equity price P_t^{eq} is given by $1 = \mathbb{E}_t \left[M_{t,t+1}^{real} e^{r_{t+1}^{eq}} \right]$, where $e^{r_{t+1}^{eq}} = (D_{t+1}^\omega + P_{t+1}^{eq}) / P_t^{eq}$, $M_{t,t+1}^{real} = M_{t,t+1} \pi_{t+1}$, and $D_t = y_t - w_t l_t - \frac{1}{2} \xi (\pi_t / \pi_{ss} - 1)^2 y_t - z_t \delta k_{ss}$. The equity premium $\mathbb{E} [r_t^{eq} - r_{t-1}^{real}]$ is 3.45% in $\mathcal{M}^{M,CS}$ without leverage (i.e. $\omega = 1$), which is somewhat lower than the corresponding empirical moment of about 6% (see, for instance, Bansal and Yaron (2004)). However, allowing for a small degree of leverage with $\omega = 2$ increases the equity premium to 6.09% in $\mathcal{M}^{M,CS}$. Thus, the proposed model is also able to explain the high equity premium in the US, although this moment was not included in the estimation.

8 Conclusion

This paper shows how to modify the New Keynesian model to generate bond return predictability from term premia dynamics that display the same satisfying properties as in reduced-form DTSMs. The key innovation is to consider a new specification for stochastic

volatility, where high current inflation increases future uncertainty. This extension enables the New Keynesian model to generate bond predictability based on the yield spread, and it ensures no return predictability in historical bond yields when adjusted for term premia. We also show that the proposed model matches the upward sloping nominal yield curve, generates an upward sloping real yield curve, produces a positive and upward sloping inflation risk premium, and explains the equity premium.

An obvious extension of our analysis is to use the proposed model as a starting point for understanding more recent bond return predictability results using macro variables, as summarized in Bauer and Hamilton (2018). Another interesting extension is to enhance our understanding of the economic forces that control the conditional volatility in bond yields by also asking the New Keynesian model to match this aspect of the data. We leave these and other extensions for future work.

A QML with Shrinkage

A.1 The Asymptotic Distribution

The asymptotic analysis is carried out based on the assumption that any filtering errors caused by the adopted integration approximation in the CDKF are small and not of relevance for the estimates. Given this assumption together with standard regularity conditions, the QML estimator based on the CDKF is consistent (see Andreasen (2013)). Standard regularity conditions also ensure that GMM is consistent, meaning that the estimator in (17) is consistent when $T \rightarrow \infty$. To derive the asymptotic distribution of $\hat{\boldsymbol{\theta}}$, note that it solves the first-order condition

$$\frac{1}{T} \sum_{t=1}^T \left(-\mathbf{s}_t(\hat{\boldsymbol{\theta}}) + 2\lambda \mathbf{G}(\hat{\boldsymbol{\theta}})' \mathbf{W} \mathbf{g}_t(\hat{\boldsymbol{\theta}}) \right) = 0.$$

A mean-value expansion of \mathbf{s}_t and \mathbf{g}_t around the true value $\boldsymbol{\theta}_o$ gives

$$-\frac{1}{T} \sum_{t=1}^T \left(\mathbf{s}_t(\boldsymbol{\theta}_o) + \tilde{\mathbf{H}}_t(\hat{\boldsymbol{\theta}} - \boldsymbol{\theta}_o) \right) + 2\lambda \mathbf{G}(\hat{\boldsymbol{\theta}})' \mathbf{W} \left(\mathbf{g}_{1:T}(\boldsymbol{\theta}_o) + \tilde{\mathbf{G}}(\hat{\boldsymbol{\theta}} - \boldsymbol{\theta}_o) \right) = 0.$$

Here, $\tilde{\mathbf{H}}_t$ is the Hessian of observation t related to the CDKF, where the tilde indicates that each row of $\tilde{\mathbf{H}}_t$ is evaluated at a different mean being on the line segment between $\boldsymbol{\theta}_o$ and $\hat{\boldsymbol{\theta}}$. Similarly, $\tilde{\mathbf{G}}$ is the Jacobian related to the shrinkage moments, where each row of $\tilde{\mathbf{G}}$ is evaluated at a different mean on the line segment between $\boldsymbol{\theta}_o$ and $\hat{\boldsymbol{\theta}}$. Simple algebra then implies

$$\hat{\boldsymbol{\theta}} - \boldsymbol{\theta}_o = \left(-\frac{1}{T} \sum_{t=1}^T \tilde{\mathbf{H}}_t + 2\lambda \mathbf{G}(\hat{\boldsymbol{\theta}})' \mathbf{W} \tilde{\mathbf{G}} \right)^{-1} \frac{1}{T} \sum_{t=1}^T \left(-\mathbf{s}_t(\boldsymbol{\theta}_o)' + 2\lambda \mathbf{G}(\hat{\boldsymbol{\theta}})' \mathbf{W} \mathbf{g}_t(\boldsymbol{\theta}_o) \right).$$

The result in Section 4.2 then follows when scaling this expression by \sqrt{T} and imposing the necessary regularity conditions for extremum estimators (see, for instance, Hayashi (2000)).

A.2 Monte Carlo Evidence

We use a simplified version of our New Keynesian model for the Monte Carlo study to keep it manageable. That is, we let $l_{ss} = 0.34$, $\phi_y = 0$, and omit labor supply shocks ($\sigma_n = 0$), shocks to the Taylor-rule ($\sigma_{\phi_\pi} = 0$), and stationary technology shocks ($\sigma_a = 0$). The New Keynesian model is solved to third order, where we use the same nine observations as contained in \mathbf{y}_t^{obs} (see Section 4.1). To study a demanding specification, we let the measurement errors have standard deviations of twice the size stated in Section 4.3, while all remaining calibrated parameters are as outlined in Section 4.3. The simulation study is carried out using 1,000 samples with $T = 250$ observations (constructed using a burn-in of 100 observations), with four observations reserved to initialize the CDKF for consistency with the results in Table 1. Case I considers the scenario, where \mathbf{v}_t is simulated by letting $\mathbf{v}_t \sim \mathcal{NID}(\mathbf{0}, \mathbf{R}_v)$ as used in the CDKF. Case II simulates \mathbf{v}_t with cross-correlation, auto-correlation, and outliers, although the CDKF is implemented using $\mathbf{v}_t \sim \mathcal{NID}(\mathbf{0}, \mathbf{R}_v)$. The simulation of \mathbf{v}_t is here done by first letting $v_{i,t}^\varepsilon = \mathcal{N}(0, 1) + 1_{\{u > 0.90\}} \times 5 + 1_{\{u < 0.10\}} \times (-5)$ for $i = 1, 2, \dots, 9$ and $t = 1, 2, \dots, T$ to generate outliers, where u is uniformly distributed on $[0, 1]$. For $\mathbf{v}_t^\varepsilon = [v_{1,t}^\varepsilon, v_{2,t}^\varepsilon, \dots, v_{9,t}^\varepsilon]'$, we then let $v_{i,t} = \rho_v v_{i,t-1} + \boldsymbol{\omega}'_t \mathbf{v}_t^\varepsilon$, where $\rho_v = 0.8$ captures auto-correlation and the column vector $\boldsymbol{\omega}$ captures cross-correlation among bond yields of the form $corr(r_t^{(n)}, r_t^{(n-1)}) = 0.99$. We then normalize $\{v_{i,t}\}_{t=1}^T$ to have zero mean and a unit variance for $i = 1, 2, \dots, 9$ in each simulated sample. To reduce the degree of simulation noise, we apply the same seeds for the random number generator used to construct the 1,000 simulated samples in Case I and II.

The results from the Monte Carlo study are summarized in Table A1. In Case I with correctly specified measurement errors in the CDKF, we find basically no biases in the QML estimates without shrinkage (i.e. $\lambda = 0$). The asymptotic normal distribution also appears to be a reasonable approximation, as most rejection probabilities (Type I errors) for testing the true null hypothesis (i.e. $\hat{\theta}_j = \theta_j^o$) at a 5% significant level are close to the nominal size. However, in Case II with misspecified measurement errors in the CDKF, we observe notable parameter biases and elevated Type I errors without shrinking the QML estimates, showing that the asymptotic standard errors in this case display a negative bias. Within this setting, shrinking (i.e. $\lambda = T$) is seen to be very beneficial, as it reduces the overall level bias in the parameters (0.049 vs. 0.059) and provides a notable improvement on the Type I errors (7.4% vs. 39.0%).

Table A1: Monte Carlo Study: Simulation Results

This table shows the performance of QML without shrinkage ($\lambda = 0$) and with shrinkage ($\lambda = T$) towards the first and second moments of \mathbf{y}_t^{obs} using 1,000 simulated samples of length $T = 250$. Case I considers the scenario, where \mathbf{v}_t is simulated by letting $\mathbf{v}_t \sim \mathcal{NID}(0, \mathbf{R}_v)$ as used in the CDKF. Case II simulates \mathbf{v}_t with cross-correlation, auto-correlation, and extreme outliers, although the CDKF is implemented using the incorrect specification $\mathbf{v}_t \sim \mathcal{NID}(0, \mathbf{R}_v)$. Level bias refers to the mean of the estimate minus the true value. The true standard error (SE) is calculated as the standard deviation of the estimates. The Type I errors are calculated at a 5 percent significance level. The overall mean absolute error (MAE) for level bias is $\frac{1}{n_\theta} \sum_{j=1}^{n_\theta} |bias_j/\theta_j|$, where θ_j refers to the true value, while for Type I overall MAE is $\frac{1}{n_\theta} \sum_{j=1}^{n_\theta} |\text{Type I}_j - 5\%|$. Here, n_θ denotes the number of elements in θ .

| | True | Level bias | | True SE | | Type I (pct.) | |
|--|-------|---------------|---------------|---------------|---------------|---------------|---------------|
| | value | $\lambda = 0$ | $\lambda = T$ | $\lambda = 0$ | $\lambda = T$ | $\lambda = 0$ | $\lambda = T$ |
| Case I: correctly specified \mathbf{v}_t | | | | | | | |
| β | 0.97 | 0.000 | 0.001 | 0.003 | 0.002 | 4.8 | 0.6 |
| χ | 6.00 | 0.013 | 0.244 | 0.281 | 0.528 | 4.8 | 0.5 |
| ϕ_π | 6.00 | 0.012 | 0.085 | 0.158 | 0.275 | 5.9 | 3.3 |
| ρ_{μ_z} | 0.973 | 0.000 | 0.001 | 0.002 | 0.002 | 5.2 | 2.2 |
| ρ_d | 0.972 | 0.000 | 0.000 | 0.001 | 0.002 | 5.9 | 1.8 |
| ρ_σ | 0.75 | -0.005 | 0.025 | 0.023 | 0.042 | 12.3 | 26.4 |
| $\sigma_{\mu_z} \times 100$ | 0.034 | 0.000 | -0.002 | 0.002 | 0.003 | 2.4 | 0.7 |
| σ_d | 0.052 | 0.000 | 0.000 | 0.001 | 0.001 | 4.5 | 2.7 |
| σ_σ | 0.01 | 0.000 | -0.001 | 0.001 | 0.003 | 7.7 | 19.2 |
| γ_π | 4.00 | 0.093 | 0.318 | 0.393 | 0.827 | 9.2 | 7.3 |
| π_{ss} | 1.021 | 0.000 | 0.000 | 0.001 | 0.000 | 13.0 | 0.5 |
| Overall MAE | - | 0.005 | 0.031 | - | - | 2.5 | 6.0 |
| Case II: misspecified \mathbf{v}_t | | | | | | | |
| β | 0.97 | 0.000 | 0.001 | 0.004 | 0.003 | 19.3 | 0.8 |
| χ | 6.00 | -0.772 | 0.020 | 0.635 | 0.592 | 65.8 | 0.9 |
| ϕ_π | 6.00 | -0.035 | 0.148 | 0.280 | 0.296 | 36.1 | 2.3 |
| ρ_{μ_z} | 0.973 | 0.002 | 0.001 | 0.002 | 0.003 | 39.6 | 4.1 |
| ρ_d | 0.972 | 0.001 | 0.001 | 0.002 | 0.002 | 29.8 | 2.7 |
| ρ_σ | 0.75 | 0.008 | 0.030 | 0.027 | 0.043 | 33.6 | 15.2 |
| $\sigma_{\mu_z} \times 100$ | 0.034 | 0.002 | -0.001 | 0.004 | 0.003 | 34.1 | 0.8 |
| σ_d | 0.052 | -0.001 | 0.000 | 0.001 | 0.001 | 46.6 | 3.2 |
| σ_σ | 0.01 | -0.004 | -0.003 | 0.001 | 0.002 | 91.2 | 51.0 |
| γ_π | 4.00 | -0.125 | 0.302 | 0.651 | 0.913 | 45.1 | 3.7 |
| π_{ss} | 1.021 | -0.001 | 0.000 | 0.001 | 0.000 | 43.2 | 0.8 |
| Overall MAE | - | 0.059 | 0.049 | - | - | 39.0 | 7.4 |

B Accuracy of Perturbation Approximation

We evaluate the accuracy of the third-order perturbation approximation by computing Euler-equation errors along a simulated sample path of 2,000 observations, which we compute using a pruned third-order perturbation approximation. The accuracy of this solution is benchmarked to a standard first-order approximation and a fourth-order approximation using the codes of Levintal (2017).²⁰ Table B1 reports the mean absolute Euler-equation errors (MAEs) for the six estimated versions of the New Keynesian model in Table 1. The results are reported in unit-free terms, meaning that a MAE of 0.1 corresponds to a 10% violation of the equilibrium equations. We clearly find that a third-order approximation improves the accuracy of the linearized solution, both for the Euler-equations relating to the macro part of the model and for the 40 Euler-equations describing bond prices. Considering a fourth order approximation provides in general no improvement in accuracy compared to the adopted third order solution.

²⁰The fifth-order perturbation approximation does not converge given the large size of our model, and hence is even less accurate than the fourth-order approximation.

Table B1: The New Keynesian Model: Euler-Equation Errors

This table reports the mean absolute unit-free Euler-equation errors (MAEs) in a first-, third-, and fourth-order perturbation approximation using a simulated sample path of 2,000 observations. For each estimated version of the New Keynesian model, the simulated sample path is computed for a pruned third-order perturbation approximation. Conditional expectations in the Euler-equations are evaluated by Gauss-Hermite quadratures using five points per shock, giving a total of $5^6 = 15,625$ points. The considered model parameters are those reported in Table 1. The MAEs to the 9 equations describing the model without bond prices are summarized under the label 'Macro Part', while the MAEs for the 40 equations describing all bond prices are summarized under the label 'Bond Prices'. The label 'Total' refers to the MAEs for the entire model.

| | $\mathcal{M}^{M,CS}$ | \mathcal{M}^M | \mathcal{M} | $\mathcal{M}_{\gamma_\pi=0}^{M,CS}$ | $\mathcal{M}_{\gamma_\pi=0}^M$ | $\mathcal{M}_{u_0=0}^{M,CS}$ |
|---------------|----------------------|-----------------|---------------|-------------------------------------|--------------------------------|------------------------------|
| Macro Part: | | | | | | |
| 1st order | 6.27 | 7.33 | 11.18 | 2.23 | 1.91 | 5.93 |
| 3rd order | 0.05 | 0.08 | 0.10 | 0.24 | 0.07 | 0.06 |
| 4th order | 0.25 | 0.40 | 0.13 | 0.23 | 0.13 | 0.23 |
| Bonds Prices: | | | | | | |
| 1st order | 26.52 | 30.99 | 45.93 | 9.10 | 7.90 | 25.26 |
| 3rd order | 0.15 | 0.24 | 0.30 | 0.72 | 0.20 | 0.19 |
| 4th order | 0.93 | 1.48 | 0.35 | 0.81 | 0.43 | 0.85 |
| Total: | | | | | | |
| 1st order | 20.69 | 24.17 | 35.88 | 7.12 | 6.17 | 19.70 |
| 3rd order | 0.12 | 0.19 | 0.24 | 0.57 | 0.16 | 0.15 |
| 4th order | 0.73 | 1.16 | 0.28 | 0.64 | 0.34 | 0.67 |

References

- Abrahams, M., Adrian, T., Crump, R. K., Moench, E. and Yu, R. (2016), ‘Decomposing Real and Nominal Yield Curves’, *Journal of Monetary Economics* **84**, 182–200.
- Adrian, T., Crump, R. K. and Moench, E. (2013), ‘Pricing the Term Structure with Linear Regressions’, *Journal of Financial Economics* **110**(1), 110–138.
- Amisano, G. and Tristani, O. (2017), ‘Monetary Policy and Long-Term Interest Rates’, *Working Paper* .
- An, S. and Schorfheide, F. (2007), ‘Bayesian Analysis of DSGE Models’, *Econometric Review* **26**(2-4), 113–172.
- Andreasen, M. M. (2012), ‘On the Effects of Rare Disasters and Uncertainty Shocks for Risk Premia in Non-Linear DSGE Models’, *Review of Economic Dynamics* **15**(3), 295–316.
- Andreasen, M. M. (2013), ‘Non-Linear DSGE Models and the Central Difference Kalman Filter’, *Journal of Applied Econometrics* **28**, 929–955.
- Andreasen, M. M., Fernandez-Villaverde, J. and Rubio-Ramirez, J. F. (2018), ‘The Pruned State Space System for Non-Linear DSGE Models: Theory and Empirical Applications to Estimation’, *Review of Economic Studies* **85**(1), 1–49.
- Andreasen, M. M. and Jørgensen, K. (forthcoming), ‘The Importance of Timing Attitudes in Consumption-Based Asset Pricing Models’, *Journal of Monetary Economics* .
- Andreasen, M. M. and Zabczyk, P. (2015), ‘Efficient Bond Price Approximations in Non-Linear Equilibrium-Based Term Structure Models’, *Studies in Nonlinear Dynamics and Econometrics* **19**(1), 1–34.
- Ang, A., Boivin, J., Dong, S. and Loo-Kung, R. (2011), ‘Monetary Policy Shifts and the Term Structure’, *Review of Economic Studies* **78**(2), 429–457.
- Bansal, R. and Shaliastovich, I. (2013), ‘A Long-Run Risks Explanation of Predictability Puzzles in Bond and Currency Markets’, *Review of Financial Studies* **26**(1), 1–33.

- Bansal, R. and Yaron, A. (2004), ‘Risks for the Long Run: A Potential Resolution of Asset Pricing Puzzles’, *Journal of Finance* **59**(4), 1481–1509.
- Barsky, R. B., Juster, F. T., Kimball, M. S. and Shapiro, M. D. (1997), ‘Preference Parameters and Behavioral Heterogeneity: An Experimental Approach in the Health and Retirement Study’, *The Quarterly Journal of Economics* pp. 537–579.
- Basu, S. and Bundick, B. (2017), ‘Uncertainty Shocks in a Model of Effective Demand’, *Econometrica* **85**(3), 937–958.
- Bauer, M. D. and Hamilton, J. D. (2018), ‘Robust Bond Risk Premia’, *Review of Financial Studies* **31**(2), 399–448.
- Bekaert, G., Cho, S. and Moreno, A. (2010), ‘New Keynesian Macroeconomics and the Term Structure’, *Journal of Money, Credit and Banking* **42**(1), 33–62.
- Bianchi, F., Kung, H. and Tirsikh, M. (2018), ‘The Orgins and Effects of Macroeconomic Uncertainty’, *NBER Working Paper 25386* .
- Binning, A. (2013), ‘Solving Second and Third-Order Approximations to DSGE Models: A Recursive Sylvester Equation Solution’, *Norges Bank, Working Paper 18* .
- Binsbergen, J. H. V., Fernandez-Villaverde, J., Koijen, R. S. and Rubio-Ramirez, J. (2012), ‘The Term Structure of Interest Rates in a DSGE Model with Recursive Preferences’, *Journal of Monetary Economics* **59**, 634–648.
- Campbell, J. Y. and Cochrane, J. H. (1999), ‘By Force of Habit: A Consumption-Based Explanation of Aggregate Stock Market Behavior’, *Journal of Political Economy* **107**(2), 205–251.
- Campbell, J. Y. and Shiller, R. J. (1991), ‘Yield Spread and Interest Rate Movements: A Bird’s Eye View’, *The Review of Economic Studies* **58**(3), 495–514.
- Cheridito, P., Filipovic, D. and Kimmel, R. L. (2007), ‘Market Price of Risk Specifications for Affine Models: Theory and Evidence’, *Journal of Financial Economics* **83**, 123–170.
- Chernov, M. and Mueller, P. (2012), ‘The term Structure of Inflation Expectations’, *Journal of Financial Economics* **106**, 367–394.

- Chernozhukov, V. and Hong, H. (2003), ‘An MCMC Approach to Classical Estimation’, *Journal of Econometrics* **115**(2), 293–346.
- Christiano, L. J., Eichenbaum, M. and Evans, C. L. (2005), ‘Nominal Rigidities and the Dynamic Effects of a Shock to Monetary Policy’, *Journal of Political Economy* **113**(1), 1–45.
- Christiano, L. J., Trabandt, M. and Walentin, K. (2011), ‘Introducing Financial Frictions and Unemployment into a Small Open Economy Model’, *Journal of Economic Dynamic and Control* **35**(12), 1999–2041.
- Cieslak, A. and Povala, P. (2015), ‘Expected Returns in Treasury Bonds’, *Review of Financial Studies* .
- Cochrane, J. H. and Piazzesi, M. (2005), ‘Bond Risk Premia’, *American Economic Review* **95**(1), 138–160.
- Coibion, O. and Gorodnichenko, Y. (2011), ‘Monetary Policy, Trend Inflation, and the Great Moderation: An Alternative Interpretation’, *American Economic Review* **101**(1), 341–370.
- Dai, Q. and Singleton, K. J. (2002), ‘Expectation Puzzles, Time-Varying Risk Premia and Affine Models of the Term Structure’, *Journal of Financial Economics* **63**(3), 415–441.
- Dew-Becker, I. (2014), ‘Bond Pricing with a Time-Varying Price of Risk in an Estimated Medium-Scale Bayesian DSGE Model’, *Journal of Money Credit and Banking* **46**(5), 837–888.
- Diebold, F. X., Rudebusch, G. D. and Aruoba, S. B. (2006), ‘The Macroeconomy and the Yield Curve: A Dynamic Latent Factor Approach’, *Journal of Econometrics* **131**, 309–338.
- Duffee, G. R. (2002), ‘Term Premia and Interest Rate Forecasts in Affine Models’, *The Journal of Finance* **57**(1), 405–443.
- Epstein, L. G., Farhi, E. and Strzalecki, T. (2014), ‘How Much Would You Pay to Resolve Long-Run Risk?’, *American Economic Review* **104**(9), 2680–2697.

- Epstein, L. G. and Zin, S. E. (1989), ‘Substitution, Risk Aversion, and the Temporal Behavior of Consumption and Asset Returns: A Theoretical Framework’, *Econometrica* **57**(4), 937–969.
- Fama, E. F. and Bliss, R. R. (1987), ‘The Information in Long-Maturity Forward Rates’, *The American Economic Review* **77**(4), 680–692.
- Fama, E. F. and French, K. R. (1989), ‘Business Conditions and Expected Returns on Stocks and Bonds’, *Journal of Financial Economics* **25**, 23–49.
- Fernández-Villaverde, J., Guerrón-Quintana, P., Kuester, K. and Rubio-Ramírez, J. (2015), ‘Fiscal Volatility Shocks and Economic Activity’, *American Economic Review* **105**(11), 3352–84.
- Fernandez-Villaverde, J., Guerron-Quintana, P., Rubio-Ramirez, J. F. and Uribe, M. (2011), ‘Risk Matters: The Real Effects of Volatility Shocks’, *American Economic Review* **101**(6), 2530–2561.
- Fernández-Villaverde, J. and Rubio-Ramírez, J. F. (2007), ‘Estimating Macroeconomic Models: A Likelihood Approach’, *Review of Economic Studies* **74**(4), 1–46.
- Fernández-Villaverde, J. and Rubio-Ramirez, J. F. (2008), ‘How Structural Are Structural Parameters?’, *2007 NBER Macroeconomic Annual* pp. 83–137.
- Graeve, F. D., Emiris, M. and Wouters, R. (2009), ‘A Structural Decomposition of the US Yield Curve’, *Journal of Monetary Economics* **56**(4), 545–559.
- Gürkaynak, R., Sack, B. and Wright, J. (2007), ‘The U.S. Treasury Yield Curve: 1961 to the Present’, *Journal of Monetary Economics* **54**, 2291–2304.
- Hall, R. E. (1988), ‘Intertemporal Substitution in Consumption’, *Journal of Political Economy* **vol**(2), 339–357.
- Hansen, L. P. (1982), ‘Large Sample Properties of Generalized Method of Moments Estimators’, *Econometrica* **50**(4), 1029–1054.
- Harvey, A. C. (1989), ‘Forecasting, Structural Time Series Models and the Kalman Filter’, *Cambridge University Press* .

- Hayashi, F. (2000), *Econometrics*, Princeton University Press, New Jersey.
- Ireland, P. N. (2004), ‘A Method for Taking Models to the Data’, *Journal of Economic Dynamics and Control* **28**(6), 1205–1226.
- Jermann, U. J. (2013), ‘A Production-Based Model for the Term Structure’, *Journal of Financial Economics* **109**(2), 293–306.
- Joslin, S., Singleton, K. J. and Zhu, H. (2011), ‘A New Perspective on Gaussian Dynamic Term Structure Models’, *The Review of Financial Studies* **24**(3), 926–970.
- Jurado, K., Ludvigson, S. and Ng, S. (2015), ‘Measuring Uncertainty’, *American Economic Review* **105**(3), 1177–1216.
- Justiniano, A. and Primiceri, G. E. (2008), ‘The Time-Varying Volatility of Macroeconomic Fluctuations’, *American Economic Review* **98**(3), 604–641.
- Keane, M. P. (2011), ‘Labor Supply and Taxes: A Survey’, *Journal of Economic Literature* **49**(4), 961–1075.
- Kliem, M. and Meyer-Gohde, A. (2017), ‘(Un)expected Monetary Policy Shocks and Term Premia’, *Bundsbank Discussion Paper No 30* .
- Kreps, D. M. and Porteus, E. L. (1978), ‘Temporal Resolution of Uncertainty and Dynamic Choice Theory’, *Econometrica* **46**(1), 185–200.
- Kung, H. (2015), ‘Macroeconomic Linkages between Monetary Policy and the Term Structure of Interest Rates’, *Journal of Financial Economics* **115**(1), 42–57.
- Levintal, O. (2017), ‘Fifth-Order Perturbation Solution to DSGE Models’, *Journal of Economics Dynamic and Control* **80**, 1–16.
- Ludvigson, S., Ma, S. and Ng, S. (2019), ‘Uncertainty and Business Cycles: Exogenous Impulse or Endogenous Response?’, *Working Paper* .
- Nakata, T. and Tanaka, H. (2016), ‘Equilibrium Yield Curves and the Interest Rate Lower Bound’, *Finance and Economic Discussion Series, Federal Reserve Board, Washington D. C.* .

- Newey, W. K. and West, K. D. (1987), ‘A Simple, Positive Semi-definite, Heteroskedasticity and Autocorrelation Consistent Covariance Matrix’, *Econometrica* **55**(3), 703–708.
- Norgaard, M., Poulsen, N. K. and Ravn, O. (2000), ‘Advances in Derivative-Free State Estimation for Nonlinear Systems’, *Automatica* **36**:11, 1627–1638.
- Rotemberg, J. J. (1982), ‘Monopolistic Price Adjustment and Aggregate Output’, *Review of Economic Studies* **49**, 517–531.
- Rudebusch, G. D. and Swanson, E. T. (2008), ‘Examining the Bond Premium Puzzle with a DSGE Model’, *Journal of Monetary Economics* **55**, 111–126.
- Rudebusch, G. D. and Swanson, E. T. (2012), ‘The Bond Premium in a DSGE Model with Long-Run Real and Nominal Risks’, *American Economic Journal: Macroeconomics* **4**(1), 1–43.
- Ruge-Murcia, F. J. (2007), ‘Methods to Estimate Dynamic Stochastic General Equilibrium Models’, *Journal of Economic Dynamics and Control* **31**(8), 2599–2636.
- Schmitt-Grohé, S. and Uribe, M. (2004), ‘Solving Dynamic General Equilibrium Models Using a Second-Order Approximation to the Policy Function’, *Journal of Economic Dynamics and Control* **28**(4), 755–775.
- Smith, J. A. A. (1993), ‘Estimating Nonlinear Time-Series Models Using Simulated Vector Autoregressions’, *Journal of Applied Econometrics* **8**, **Supplement: Special Issue on Econometric Inference Using Simulation Techniques**, S63–S84.
- Swanson, E. T. (2018), ‘Risk Aversion, Risk Premia, and the Labor Margin with Generalized Recursive Preferences’, *Review of Economic Dynamics* **28**, 290–321.
- Wachter, J. A. (2006), ‘A Consumption-Based Model of the Term Structure of Interest Rates’, *Journal of Financial Economics* **79**(2), 365–399.
- Weil, P. (1990), ‘Unexpected Utility in Macroeconomics’, *Quarterly Journal of Economics* **105**(1), 29–42.
- Yogo, M. (2004), ‘Estimating the Elasticity of Intertemporal Substitution When Instruments Are Weak’, *The Review of Economics and Statistics* **86**(3), 797–810.

Figure 1: Model Fit

This figure shows the fit of $\mathcal{M}^{M,CS}$ when evaluated at the posterior state estimates from the CDKF using US data from 1961 Q2 to 2016 Q2.

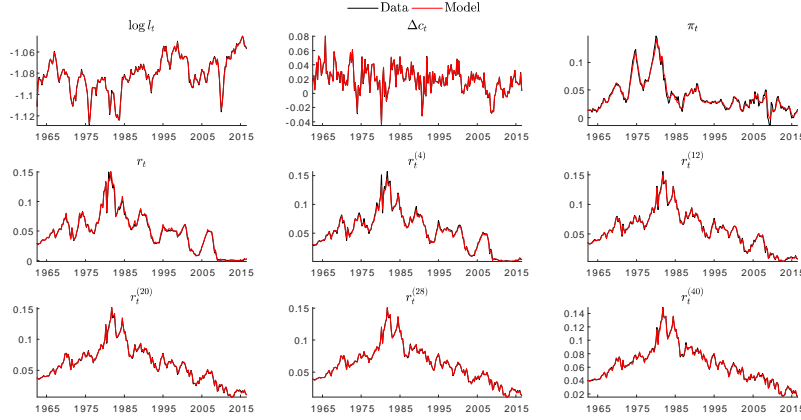


Figure 2: The Campbell-Shiller Loadings

This figure shows the Campbell-Shiller regression loadings β_k for $m = 4$ in US data from 1961 Q2 to 2016 Q2. The shaded area denotes the 95 percent confidence interval for these estimates, computed with a block bootstrap where the regressand and the regressor in (1) are sampled jointly in blocks of 10 observations in 100,000 bootstrap samples. The model-implied Campbell-Shiller moments are computed in closed form based on Andreasen et al. (2018).

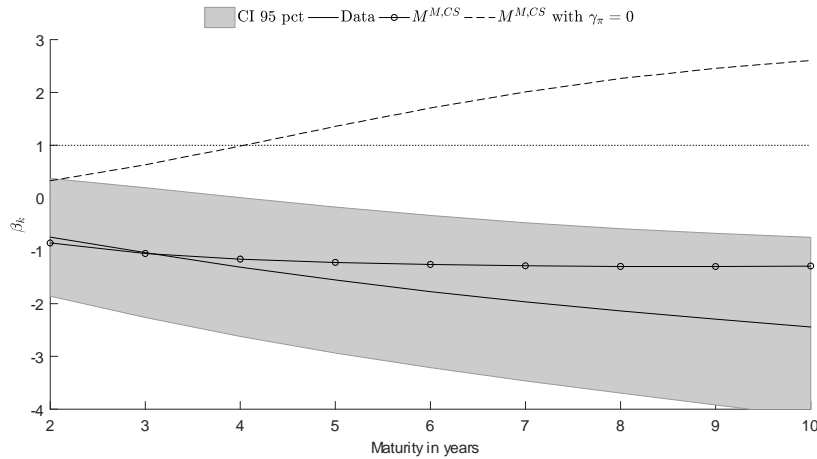


Figure 3: Risk-Adjusted Campbell-Shiller Loadings

The figure shows the risk-adjusted Campbell-Shiller regression loadings β_k^{Adj} for $m = 4$ in US data from 1961 Q2 to 2016 Q2 when using the term premium from $\mathcal{M}^{M,CS}$. The shaded area denotes the 95 percent confidence interval for these estimates, computed with a block bootstrap where the regressand and the regressor in (18) are sampled jointly in blocks of 10 observations in 100,000 bootstrap samples.

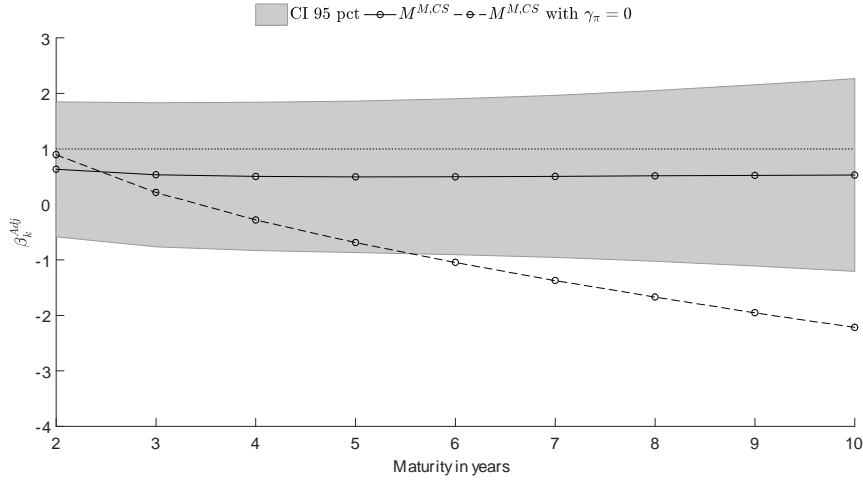


Figure 4: The Ten-year Nominal Term Premia

This figure shows the ten-year nominal term premium in annualized basis points from $\mathcal{M}^{M,CS}$ and the model by Adrian et al. (2013). The gray shaded bars denote NBER recessions.

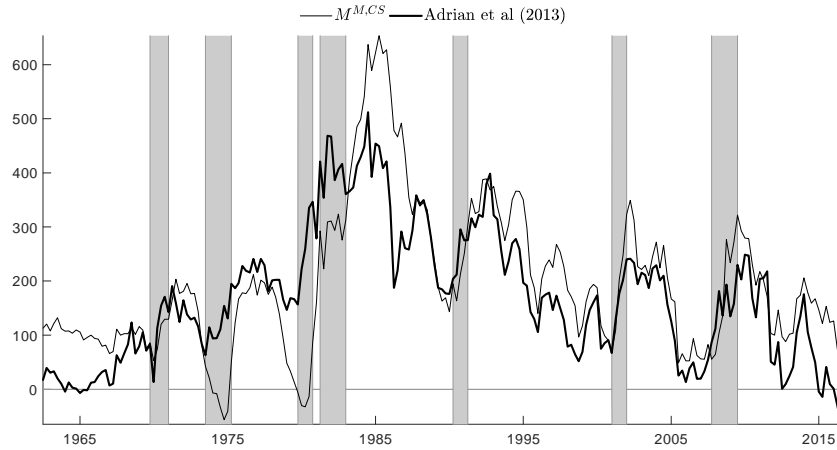


Figure 5: Impulse Response Functions: Permanent Productivity Shock

This figure shows the effects of a positive one-standard deviation shock to $v_{\mu_z,t}$ computed at the ergodic mean of the states using the results in Andreasen et al. (2018). Except for $M_{t,t+1}$, all impulse response functions are scaled by 100, with consumption expressed in deviations from the balanced growth path.

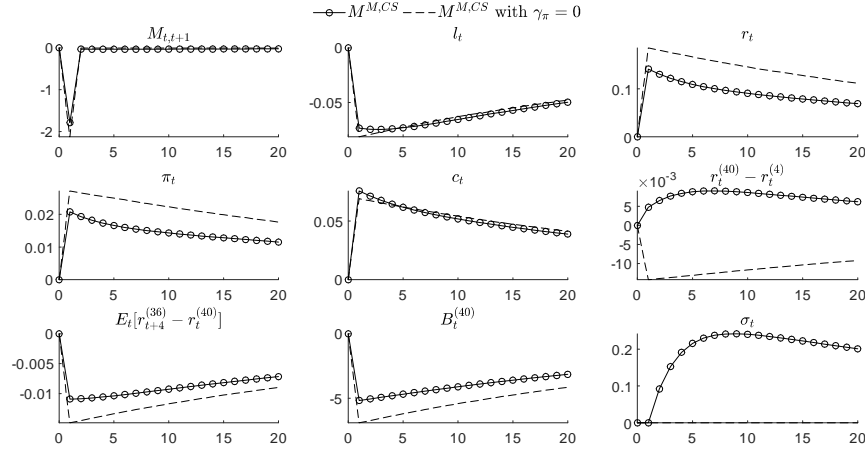


Figure 6: Impulse Response Functions: Preference Shock

This figure shows the effects of a positive one-standard deviation shock to $v_{d,t}$ computed at the ergodic mean of the states using the results in Andreasen et al. (2018). Except for $M_{t,t+1}$, all impulse response functions are scaled by 100, with consumption expressed in deviations from the balanced growth path.

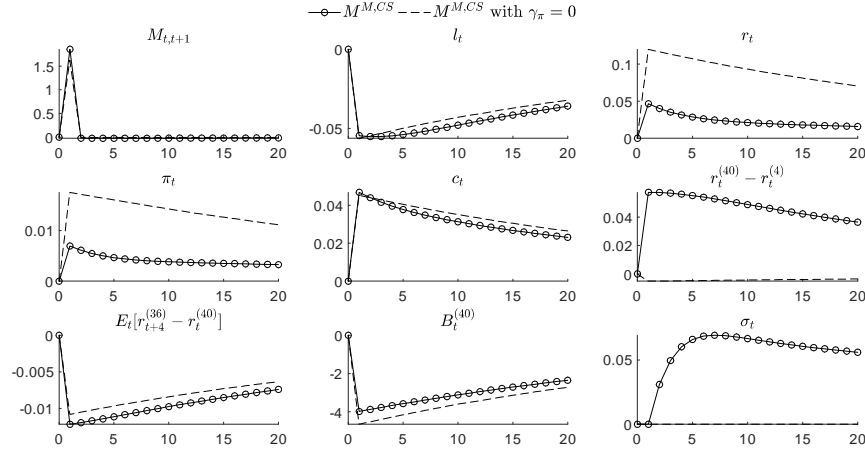


Figure 7: Impulse Response Functions for Standard Yield Curve Factors

This figure shows the impulse response functions for the level, slope, and curvature factor of the yield curve following a positive one-standard deviation disturbance to each of the structural shocks in $\mathcal{M}^{M,CS}$. The impulse response functions are computed at the ergodic mean of the states using the results in Andreasen et al. (2018).

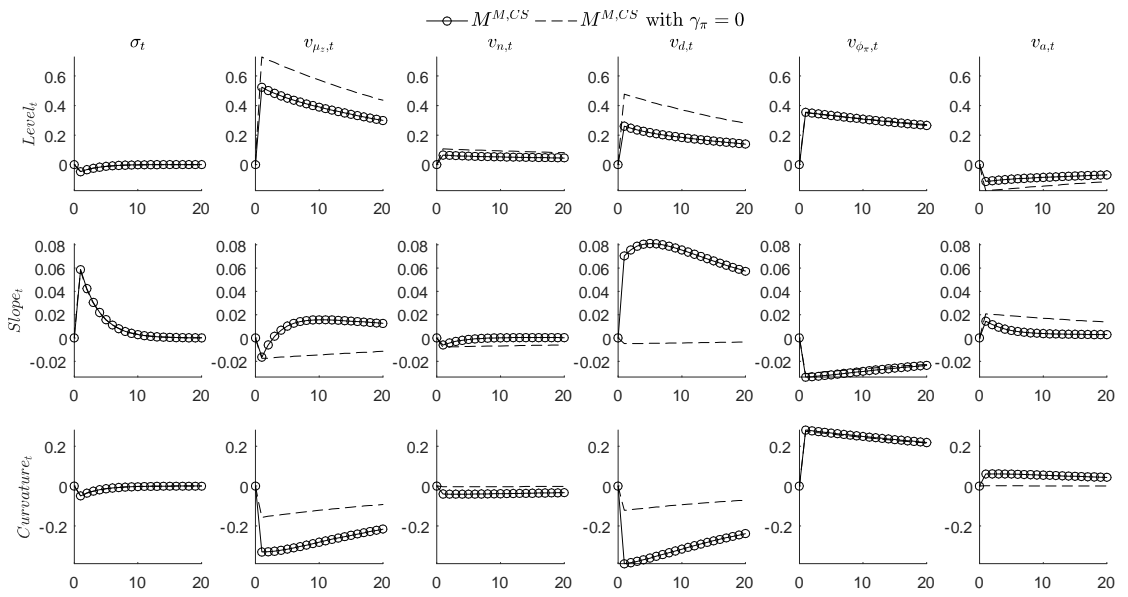


Figure 8: The Ten-year Nominal Term Premia: A Shock Decomposition

This figure shows how each of the structural shocks in $\mathcal{M}^{M,CS}$ contributes to the variation in the ten-year nominal term premium. The percentage of the total variation in the nominal term premium explained by each shock, denoted $\text{pct}(\Delta TP_t)$, is computed based on the absolute variation in the series. The gray shaded bars denote NBER recessions, and term premium is expressed in annualized basis points.

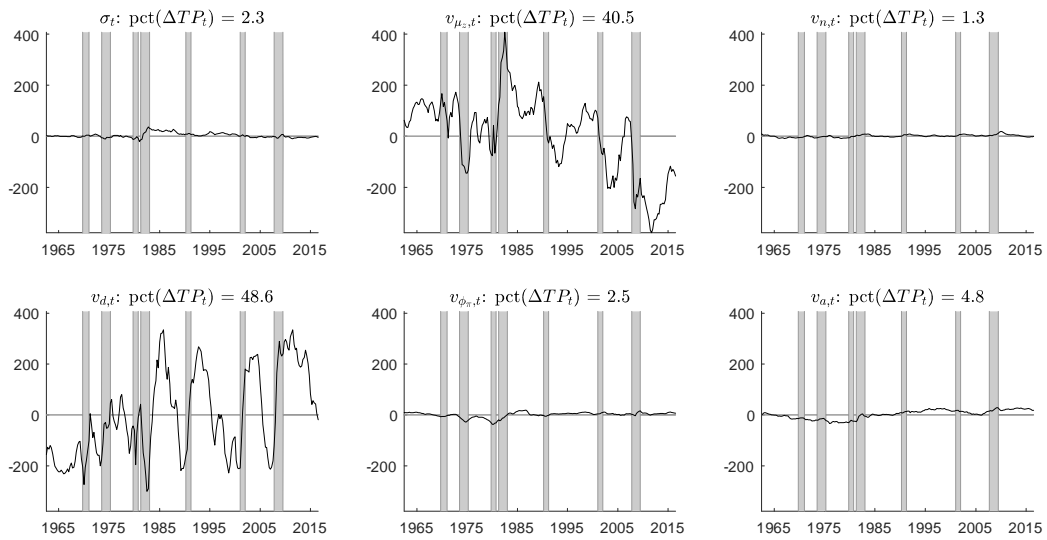


Table 1: The New Keynesian Model: The Structural Parameters

Estimation results using data from 1961 Q2 to 2016 Q2, with asymptotic standard errors provided in parenthesis. The first four observations are used to initialize the CDKF. When shrinkage is applied in the estimation, as denoted by the superscripts M and CS on the model object \mathcal{M} , an equal weighting between moments related to the three macro variables (i.e. $\log l_t$, Δc_t , and π_t) and moments related to the yield curve (i.e. six bond yields and six moments to capture the three Campbell-Shiller loadings) is targeted by correcting for the number of included moments. Hence, for $\mathcal{M}^{M,CS}$, $\mathcal{M}_{\gamma_\pi=0}^{M,CS}$, and $\mathcal{M}_{u_0=0}^{M,CS}$, the weights assigned to each of the macro moments are upscaled by four, whereas they are upscaled by two for \mathcal{M}^M . No standard error is provided for ϕ_y in the case of $\mathcal{M}_{u_0=0}^{M,CS}$, because this parameter is at its lower bound. The timing premium is evaluated at the steady state and computed as in Andreasen and Jørgensen (forthcoming).

| | Full model | | | Reduced model | | |
|-----------------------------|----------------------|------------------|-------------------|-------------------------------------|--------------------------------|------------------------------|
| | $\mathcal{M}^{M,CS}$ | \mathcal{M}^M | \mathcal{M} | $\mathcal{M}_{\gamma_\pi=0}^{M,CS}$ | $\mathcal{M}_{\gamma_\pi=0}^M$ | $\mathcal{M}_{u_0=0}^{M,CS}$ |
| l_{ss} | 0.340 (0.001) | 0.340 (0.001) | 0.315 (0.013) | 0.340 (0.001) | 0.340 (0.001) | 0.34 (0.001) |
| β | 0.967 (0.007) | 0.966 (0.004) | 0.975 (0.008) | 0.985 (0.002) | 0.992 (0.004) | 0.967 (0.006) |
| χ | 6.672 (1.168) | 7.288 (0.607) | 11.732 (0.819) | 6.422 (0.050) | 7.903 (0.021) | 6.650 (0.961) |
| ϕ_π | 6.926 (0.729) | 7.190 (0.633) | 5.187 (0.384) | 3.856 (0.121) | 4.620 (0.015) | 7.923 (0.64) |
| ϕ_y | 0.025 (0.088) | 0.097 (0.053) | 0.194 (0.062) | 0.081 (0.069) | 0.099 (0.009) | 0.000 – |
| ρ_{μ_z} | 0.973 (0.004) | 0.962 (0.004) | 0.973 (0.003) | 0.988 (0.001) | 0.972 (0.003) | 0.971 (0.005) |
| ρ_n | 0.985 (0.015) | 0.982 (0.015) | 0.990 (0.004) | 0.997 (0.005) | 0.995 (0.003) | 0.96 (0.009) |
| ρ_d | 0.972 (0.004) | 0.962 (0.003) | 0.975 (0.004) | 0.976 (0.002) | 0.971 (0.002) | 0.975 (0.006) |
| ρ_{ϕ_π} | 0.987 (0.01) | 0.974 (0.008) | 0.917 (0.007) | 0.911 (0.019) | 0.900 (0.010) | 0.986 (0.009) |
| ρ_a | 0.977 (0.011) | 0.951 (0.006) | 0.966 (0.003) | 0.998 (0.006) | 0.995 (0.005) | 0.957 (0.013) |
| ρ_σ | 0.724 (0.035) | 0.722 (0.021) | 0.624 (0.039) | 0.864 (0.031) | 0.911 (0.014) | 0.715 (0.036) |
| π_{ss} | 1.021 (0.002) | 1.021 (0.002) | 1.030 (0.003) | 1.026 (0.002) | 1.022 (0.002) | 1.019 (0.002) |
| $\sigma_{\mu_z} \times 100$ | 0.034 (0.001) | 0.040 (0.001) | 0.022 (0.001) | 0.019 (0.001) | 0.020 (0.001) | 0.034 (0.001) |
| σ_n | 0.043 (0.007) | 0.045 (0.007) | 0.072 (0.006) | 0.035 (0.009) | 0.045 (0.007) | 0.043 (0.008) |
| σ_d | 0.052 (0.004) | 0.055 (0.002) | 0.052 (0.002) | 0.045 (0.001) | 0.046 (0.001) | 0.045 (0.004) |
| σ_{ϕ_π} | 0.080 (0.044) | 0.125 (0.017) | 0.091 (0.012) | 0.103 (0.03) | 0.195 (0.039) | 0.101 (0.052) |
| σ_a | 0.004 (0.001) | 0.004 (0.001) | 0.011 (0.002) | 0.004 (0.001) | 0.004 (0.001) | 0.004 (0.001) |
| σ_σ | 0.010 (0.005) | 0.024 (0.005) | 0.015 (0.003) | 0.009 (0.003) | 0.016 (0.004) | 0.011 (0.005) |
| γ_π | 4.455 (0.475) | 6.037 (1.313) | 2.222 (0.361) | – | – | 4.861 (0.149) |
| Timing Premium | 9% | 8% | 4% | 10% | 7% | 9% |
| IES | 0.15 | 0.14 | 0.09 | 0.16 | 0.13 | 0.15 |
| RRA | 10 | 10 | 10 | 10 | 10 | 217 |
| u_0 | –3.75 | –3.54 | –4.54 | –3.84 | –3.32 | 0 |

Table 2: Goodness of Insample Fit

Panel A shows the standard deviations of the measurement errors computed using the posterior state estimates from the CDKF. Panel B shows a decomposition of the objective function $\mathcal{L} \equiv \mathcal{L}^{CDKF} + Q^{GMM}$, where $\mathcal{L}^{CDKF} \equiv \frac{1}{T} \sum_{t=1}^T \mathcal{L}_t(\boldsymbol{\theta})$ and $Q^{GMM} \equiv -\lambda \mathbf{g}_{1:T}(\boldsymbol{\theta})' \mathbf{W} \mathbf{g}_{1:T}(\boldsymbol{\theta})$.

| | Full model | | | Reduced model | | |
|------------------------------|----------------------|-----------------|---------------|-------------------------------------|--------------------------------|------------------------------|
| | $\mathcal{M}^{M,CS}$ | \mathcal{M}^M | \mathcal{M} | $\mathcal{M}_{\gamma_\pi=0}^{M,CS}$ | $\mathcal{M}_{\gamma_\pi=0}^M$ | $\mathcal{M}_{u_0=0}^{M,CS}$ |
| Panel A: Measurement errors | | | | | | |
| $std(\log l_t)$ | 7.8 | 7.3 | 3.5 | 10.0 | 7.2 | 7.6 |
| $std(\Delta c_t)$ | 5.1 | 9.0 | 6.7 | 22.9 | 11.6 | 4.7 |
| $std(\pi_t)$ | 48.1 | 37.5 | 12.9 | 23.4 | 13.4 | 46.9 |
| $std(r_t)$ | 20.1 | 27.4 | 13.8 | 26.3 | 24.7 | 21.5 |
| $std\left(r_t^{(4)}\right)$ | 23.8 | 24.0 | 18.4 | 33.2 | 27.8 | 26.6 |
| $std\left(r_t^{(12)}\right)$ | 14.3 | 13.8 | 10.4 | 24.3 | 19.8 | 14.9 |
| $std\left(r_t^{(20)}\right)$ | 9.6 | 10.7 | 8.8 | 11.4 | 9.0 | 10.5 |
| $std\left(r_t^{(28)}\right)$ | 8.1 | 7.2 | 5.3 | 8.6 | 7.7 | 8.7 |
| $std\left(r_t^{(40)}\right)$ | 13.0 | 13.4 | 9.6 | 17.4 | 17.6 | 13.6 |
| Panel B: Objective function | | | | | | |
| \mathcal{L}^{CDKF} | 33.4 | 34.6 | 35.8 | 30.8 | 33.1 | 33.4 |
| Q^{GMM} | -1.9 | -0.4 | 0.0 | -4.6 | -0.5 | -1.8 |
| \mathcal{L} | 31.5 | 34.2 | 35.8 | 26.2 | 32.6 | 31.6 |

Table 3: Unconditional First and Second Moments

The data moments are for the US from 1961 Q2 to 2016 Q2 with 95% confidence bands stated below. These bands are computed using a block bootstrap with 100,000 bootstrap samples using blocks of 60 observations. The model-implied moments are computed in closed form based on Andreasen et al. (2018). Except for $\mathbb{E}[\log l_t]$, all means and standard deviations are stated in annualized percent.

| | Data | Full model | | | Reduced model | | |
|--------------|------------------------|----------------------|-----------------|---------------|-------------------------------------|--------------------------------|------------------------------|
| | | $\mathcal{M}^{M,CS}$ | \mathcal{M}^M | \mathcal{M} | $\mathcal{M}_{\gamma_\pi=0}^{M,CS}$ | $\mathcal{M}_{\gamma_\pi=0}^M$ | $\mathcal{M}_{u_0=0}^{M,CS}$ |
| Means | | | | | | | |
| $\log l_t$ | -1.08 [-1.09,-1.07] | -1.08 | -1.08 | -1.16 | -1.08 | -1.08 | -1.08 |
| Δc_t | 1.94 [1.42,2.47] | 1.96 | 1.96 | 1.95 | 1.94 | 1.94 | 1.95 |
| π_t | 3.88 [2.00,5.77] | 4.00 | 3.89 | 4.85 | 4.10 | 3.93 | 3.99 |
| r_t | 4.76 [2.45,7.07] | 4.89 | 4.88 | 8.28 | 4.70 | 4.87 | 4.92 |
| $r_t^{(4)}$ | 5.24 [2.75,7.73] | 5.10 | 5.10 | 8.36 | 5.03 | 5.07 | 5.12 |
| $r_t^{(12)}$ | 5.64 [3.18,8.10] | 5.55 | 5.55 | 8.51 | 5.66 | 5.52 | 5.54 |
| $r_t^{(20)}$ | 5.92 [3.55,8.28] | 5.85 | 5.86 | 8.57 | 6.02 | 5.86 | 5.84 |
| $r_t^{(28)}$ | 6.13 [3.85,8.40] | 6.06 | 6.09 | 8.59 | 6.16 | 6.13 | 6.05 |
| $r_t^{(40)}$ | 6.35 [4.18,8.52] | 6.25 | 6.33 | 8.59 | 6.03 | 6.42 | 6.28 |
| Stds | | | | | | | |
| $\log l_t$ | 1.72 [1.42,2.02] | 2.53 | 2.29 | 5.05 | 5.05 | 4.59 | 1.72 |
| π_t | 1.79 [1.55,2.04] | 1.93 | 1.95 | 2.63 | 1.96 | 1.98 | 1.93 |
| Δc_t | 2.91 [1.54,4.27] | 2.87 | 3.11 | 2.43 | 2.38 | 2.94 | 2.92 |
| r_t | 3.17 [2.11,4.23] | 3.53 | 3.57 | 4.27 | 3.18 | 3.62 | 3.46 |
| $r_t^{(4)}$ | 3.30 [2.20,4.41] | 3.49 | 3.33 | 4.20 | 3.25 | 3.48 | 3.43 |
| $r_t^{(12)}$ | 3.14 [2.03,4.24] | 3.57 | 3.29 | 4.17 | 3.49 | 3.29 | 3.54 |
| $r_t^{(20)}$ | 2.97 [1.88,4.06] | 3.64 | 3.33 | 4.14 | 3.71 | 3.18 | 3.62 |
| $r_t^{(28)}$ | 2.84 [1.76,3.91] | 3.66 | 3.30 | 4.09 | 3.88 | 3.08 | 3.65 |
| $r_t^{(40)}$ | 2.70 [1.65,3.76] | 3.61 | 3.18 | 3.95 | 4.08 | 2.92 | 3.59 |

Table 4: Decomposing the Effects of the Structural Shocks

This table reports unconditional moments for $\mathcal{M}^{M,CS}$ when all structural shocks are present in column (1), and when each of the structural shocks are omitted in columns (2) to (7). The model-implied moments are computed in closed form based on Andreasen et al. (2018). Except for $\mathbb{E}[\log l_t]$, all means and standard deviations are stated in annualized percent.

| | (1) Benchmark | (2) $\sigma_\sigma = 0$ | (3) $\sigma_{\mu_z} = 0$ | (4) $\sigma_n = 0$ | (5) $\sigma_d = 0$ | (6) $\sigma_{\phi_\pi} = 0$ | (7) $\sigma_a = 0$ |
|-----------------------------|----------------------|----------------------------|-----------------------------|-----------------------|-----------------------|--------------------------------|-----------------------|
| Means | | | | | | | |
| $\log l_t$ | -1.08 | -1.08 | -1.08 | -1.08 | -1.08 | -1.08 | -1.08 |
| Δc_t | 1.96 | 1.96 | 1.94 | 1.96 | 1.96 | 1.96 | 1.96 |
| π_t | 4.00 | 4.00 | 3.26 | 4.04 | 8.97 | 4.00 | 4.04 |
| r_t | 4.89 | 4.89 | -0.27 | 5.17 | 39.34 | 4.89 | 5.19 |
| $r_t^{(4)}$ | 5.10 | 5.10 | 1.96 | 5.37 | 37.34 | 5.10 | 5.39 |
| $r_t^{(12)}$ | 5.55 | 5.55 | 7.32 | 5.80 | 32.47 | 5.55 | 5.80 |
| $r_t^{(20)}$ | 5.85 | 5.85 | 11.93 | 6.09 | 28.21 | 5.85 | 6.08 |
| $r_t^{(28)}$ | 6.06 | 6.06 | 15.91 | 6.28 | 24.48 | 6.06 | 6.27 |
| $r_t^{(40)}$ | 6.25 | 6.25 | 20.90 | 6.44 | 19.72 | 6.25 | 6.42 |
| Stds | | | | | | | |
| $\log l_t$ | 2.53 | 2.53 | 2.52 | 1.30 | 2.47 | 2.52 | 2.29 |
| π_t | 1.93 | 1.93 | 1.78 | 1.58 | 1.96 | 1.92 | 1.47 |
| Δc_t | 2.87 | 2.87 | 3.19 | 2.85 | 1.29 | 0.63 | 2.84 |
| r_t | 3.53 | 3.50 | 2.68 | 3.49 | 5.20 | 2.44 | 3.46 |
| $r_t^{(4)}$ | 3.49 | 3.48 | 2.42 | 3.46 | 4.95 | 2.45 | 3.43 |
| $r_t^{(12)}$ | 3.57 | 3.57 | 2.07 | 3.55 | 4.31 | 2.70 | 3.53 |
| $r_t^{(20)}$ | 3.64 | 3.64 | 1.94 | 3.62 | 3.79 | 2.89 | 3.60 |
| $r_t^{(28)}$ | 3.66 | 3.66 | 1.89 | 3.64 | 3.39 | 2.99 | 3.63 |
| $r_t^{(40)}$ | 3.61 | 3.61 | 1.86 | 3.59 | 2.95 | 3.03 | 3.58 |
| CS loadings | | | | | | | |
| β_{12} | -1.05 | -1.23 | -0.66 | -1.12 | 0.14 | -1.27 | -1.13 |
| β_{20} | -1.22 | -1.33 | -0.77 | -1.27 | 0.17 | -1.50 | -1.30 |
| β_{28} | -1.28 | -1.37 | -0.77 | -1.34 | 0.21 | -1.65 | -1.37 |
| β_{40} | -1.29 | -1.36 | -0.74 | -1.34 | 0.26 | -1.83 | -1.38 |
| Adjusted CS loadings | | | | | | | |
| β_{12}^{Adj} | 0.53 [-0.76,1.83] | 0.50 [-0.83,1.83] | -1.27 [-3.02,0.48] | 0.98 [-0.39,2.35] | -0.35 [-1.67,0.97] | -0.34 [-1.63,0.95] | 0.39 [-0.75,1.53] |
| β_{20}^{Adj} | 0.50 [-0.87,1.86] | 0.62 [-0.91,2.16] | -1.10 [-3.38,1.19] | 1.20 [-0.28,2.68] | -0.81 [-2.38,0.75] | -0.44 [-1.84,0.96] | 0.41 [-0.80,1.63] |
| β_{28}^{Adj} | 0.51 [-0.96,1.97] | 0.73 [-1.02,2.47] | -1.23 [-3.88,1.42] | 1.45 [-0.16,3.06] | -1.11 [-2.91,0.70] | -0.48 [-1.92,0.96] | 0.47 [-0.90,1.84] |
| β_{40}^{Adj} | 0.53 [-1.21,2.27] | 0.89 [-1.28,3.05] | -1.66 [-4.67,1.36] | 1.74 [-0.25,3.74] | -1.37 [-3.55,0.81] | -0.50 [-2.06,1.07] | 0.55 [-1.21,2.31] |

Table 5: Decomposing Conditional Standard Deviations

This table reports the standard deviation of $\sigma_{\mathbf{y}^{obs},t}$ in a simulated sample of 10,000 observations, where $\sigma_{\mathbf{y}^{obs},t}$ denotes the conditional standard deviation of \mathbf{y}_{t+1}^{obs} given \mathbf{x}_t . The quarterly conditional standard deviations are not annualized. Column (1) reports $\text{std}(\sigma_{\mathbf{y}^{obs},t})$ in basis points for $\mathcal{M}^{M,CS}$. Column (2) reports the percentage change in $\text{std}(\sigma_{\mathbf{y}^{obs},t})$ compared column (1) when imposing $\gamma_\pi = 0$ in $\mathcal{M}^{M,CS}$. Column (3) reports the percentage change in $\text{std}(\sigma_{\mathbf{y}^{obs},t})$ compared to column (1) when imposing $\gamma_\pi = 0$ and $\sigma_\sigma = 0$ in $\mathcal{M}^{M,CS}$.

| | (1) $\text{std}(\sigma_{\mathbf{y}^{obs},t})$ in bps | (2) Pct change in $\text{std}(\sigma_{\mathbf{y}^{obs},t})$ when $\gamma_\pi = 0$ | (3) Pct change in $\text{std}(\sigma_{\mathbf{y}^{obs},t})$ when $\gamma_\pi = 0$ and $\sigma_\sigma = 0$ |
|--------------|--|---|---|
| l_t | 0.44 | 7% | -1% |
| Δc_t | 0.68 | -43% | -47% |
| π_t | 1.48 | -6% | -8% |
| r_t | 2.68 | -49% | -60% |
| $r_t^{(4)}$ | 1.68 | -38% | -41% |
| $r_t^{(12)}$ | 1.36 | -42% | -41% |
| $r_t^{(20)}$ | 1.21 | -46% | -46% |
| $r_t^{(28)}$ | 1.04 | -48% | -48% |
| $r_t^{(40)}$ | 0.82 | -48% | -48% |

Table 6: Ordinary and Risk-Adjusted Campbell-Shiller Loadings

The first part of the table shows the Campbell-Shiller regression loadings β_k for $m = 4$. The moments in the data are computed from 1961 Q2 to 2016 Q2, with the 95 percent confidence interval (shown below the estimate) computed using a block bootstrap, where the regressand and the regressor in (1) are sampled jointly in blocks of 10 observations in 100,000 bootstrap samples. The model-implied Campbell-Shiller moments are computed in closed form based on Andreasen et al. (2018). The second part of the table shows the risk-adjusted Campbell-Shiller regression loadings β_k^{Adj} for $m = 4$ computed using term premia from the indicated version of the New Keynesian model and US bond yields from 1961 Q2 to 2016 Q2. The 95 percent confidence interval is reported below the point estimate of β_k^{Adj} and computed using a block bootstrap, where the regressand and the regressor in (18) are sampled jointly in blocks of 10 observations in 100,000 bootstrap samples.

| | Data | Full model | | | Reduced model | | |
|-----------------------------|------------------------|----------------------|----------------------|----------------------|-------------------------------------|--------------------------------|------------------------------|
| | | $\mathcal{M}^{M,CS}$ | \mathcal{M}^M | \mathcal{M} | $\mathcal{M}_{\gamma_\pi=0}^{M,CS}$ | $\mathcal{M}_{\gamma_\pi=0}^M$ | $\mathcal{M}_{u_0=0}^{M,CS}$ |
| CS loadings | | | | | | | |
| β_{12} | -1.03 [-2.27,0.20] | -1.05 | -0.59 | -0.20 | -0.61 | 0.39 | -1.17 |
| β_{20} | -1.55 [-2.94,-0.16] | -1.22 | -0.71 | -0.32 | -0.82 | 0.53 | -1.32 |
| β_{28} | -1.96 [-3.47,-0.46] | -1.28 | -0.74 | -0.32 | -0.99 | 0.70 | -1.36 |
| β_{40} | -2.44 [-4.14,-0.74] | -1.29 | -0.69 | -0.25 | -1.19 | 0.96 | -1.32 |
| Adjusted CS loadings | | | | | | | |
| β_{12}^{Adj} | - | 0.53 [-0.76,1.83] | 1.02 [-0.28,2.33] | 0.12 [-1.25,1.49] | -0.36 [-1.69,0.98] | -0.27 [-1.76,1.22] | 0.84 [-0.37,2.04] |
| β_{20}^{Adj} | - | 0.50 [-0.87,1.86] | 0.99 [-0.30,2.28] | 0.18 [-1.25,1.60] | -0.93 [-2.27,0.42] | -0.82 [-2.42,0.79] | 0.83 [-0.43,2.09] |
| β_{28}^{Adj} | - | 0.51 [-0.96,1.97] | 1.01 [-0.32,2.34] | 0.32 [-1.10,1.74] | -1.25 [-2.53,0.03] | -1.18 [-2.82,0.46] | 0.85 [-0.53,2.23] |
| β_{40}^{Adj} | - | 0.53 [-1.21,2.27] | 1.02 [-0.52,2.55] | 0.59 [-0.86,2.04] | -1.49 [-2.69,-0.28] | -1.50 [-3.23,0.22] | 0.85 [-0.86,2.56] |

Table 7: Reduced-Form Volatility Regressions

Model I estimates $\sigma_{t+1} = \alpha + \rho_1\sigma_t + \gamma_\pi\pi_t + \varepsilon_{t+1}$ using OLS and Newey-West standard errors implemented with 6 lags. Model II estimates $\sigma_{t+1} = \alpha + \rho_1\sigma_t + \rho_2\sigma_{t-1} + \gamma_\pi\pi_t + \varepsilon_{t+1}$ using OLS and White's heteroskedastic-consistent standard errors. The standard errors are reported in parenthesis. For both models, uncertainty σ_t is measured by the monthly macro uncertainty index of Jurado et al. (2015) one month ahead, and inflation π_t is measured monthly by the yearly change in all items for the consumer price index for all urban consumers, divided by 1200. Significance at the 10 and 5 percent level is denoted by * and **, respectively.

| | Model I | | | Model II | | | |
|------------------|-------------------|--------------------|-------------------|--------------------|---------------------|--------------------|--------------------|
| | α | ρ_1 | γ_π | α | ρ_1 | ρ_2 | γ_π |
| 1961:7 to 2015:4 | 0.014 (0.011) | 0.972** (0.020) | 1.27** (0.604) | 0.016** (0.005) | -0.619** (0.053) | 1.591** (0.058) | 0.752** (0.258) |
| 1990:1 to 2015:4 | -0.003 (0.019) | 0.991** (0.027) | 4.203* (2.157) | 0.011 (0.007) | -0.688 (0.077) | 1.668 (0.085) | 1.148** (0.570) |

Research Papers 2019



- 2018-32: Sebastian Ankargren, Måns Unosson and Yukai Yang: A mixed-frequency Bayesian vector autoregression with a steady-state prior
- 2018-33: Carlos Vladimir Rodríguez-Caballero and Massimiliano Caporin: A multilevel factor approach for the analysis of CDS commonality and risk contribution
- 2018-34: James G. MacKinnon, Morten Ørregaard Nielsen, David Roodman and Matthew D. Webb: Fast and Wild: Bootstrap Inference in Stata Using boottest
- 2018-35: Sepideh Dolatabadim, Paresh Kumar Narayan, Morten Ørregaard Nielsen and Ke Xu: Economic significance of commodity return forecasts from the fractionally cointegrated VAR model
- 2018-36: Charlotte Christiansen, Niels S. Grønberg and Ole L. Nielsen: Mutual Fund Selection for Realistically Short Samples
- 2018-37: Niels S. Grønberg, Asger Lunde, Kasper V. Olesen and Harry Vander Elst: Realizing Correlations Across Asset Classes
- 2018-38: Riccardo Borghi, Eric Hillebrand, Jakob Mikkelsen and Giovanni Urga: The dynamics of factor loadings in the cross-section of returns
- 2019-01: Andrea Gatto and Francesco Busato: Defining, measuring and ranking energy vulnerability
- 2019-02: Federico Carlini and Paolo Santucci de Magistris: Resuscitating the co-fractional model of Granger (1986)
- 2019-03: Martin M. Andreasen and Mads Dang: Estimating the Price Markup in the New Keynesian Model
- 2019-04: Daniel Borup, Bent Jesper Christensen and Yunus Emre Ergemen: Assessing predictive accuracy in panel data models with long-range dependence
- 2019-05: Antoine A. Djogbenou, James G. MacKinnon and Morten Ørregaard Nielsen: Asymptotic Theory and Wild Bootstrap Inference with Clustered Errors
- 2019-06: Vanessa Berenguer-Rico, Søren Johansen and Bent Nielsen: The analysis of marked and weighted empirical processes of estimated residuals
- 2019-07: Søren Kjærgaard, Yunus Emre Ergemen, Kallestrup-Lamb, Jim Oeppen and Rune Lindahl-Jacobsen: Forecasting Causes of Death using Compositional Data Analysis: the Case of Cancer Deaths
- 2019-08: Søren Kjærgaard, Yunus Emre Ergemen, Marie-Pier Bergeron Boucher, Jim Oeppen and Malene Kallestrup-Lamb: Longevity forecasting by socio-economic groups using compositional data analysis
- 2019-09: Debopam Bhattacharya, Pascaline Dupas and Shin Kanaya: Demand and Welfare Analysis in Discrete Choice Models with Social Interactions
- 2019-10: Martin Møller Andreasen, Kasper Jørgensen and Andrew Meldrum: Bond Risk Premiums at the Zero Lower Bound
- 2019-11: Martin Møller Andrasen: Explaining Bond Return Predictability in an Estimated New Keynesian Model